TAMPERE UNIVERSITY OF TECHNOLOGY

DANI KORPI

Analog Imperfections in Wireless Full-Duplex Transceivers

Master of Science Thesis

Supervisors: M.Sc. Taneli Riihonen
D.Sc. Lauri Anttila
Examiner: Prof. Mikko Valkama

Examiner and topic approved in the council meeting
of Faculty of Computing and Electrical Engineering
on 4.12.2013

ABSTRACT

TAMPERE UNIVERSITY OF TECHNOLOGY
Master's Degree Programme in Signal Processing and Communications Engineering
KORPI, DANI: Analog Imperfections in Wireless Full-Duplex Transceivers
Master of Science Thesis, 65 pages, 4 Appendix pages
February 2014
Major: Wireless Communications
Supervisors: M.Sc. Taneli Riihonen and D.Sc. Lauri Anttila
Examiner: Prof. Mikko Valkama
Keywords: full-duplex, nonlinear distortion, analog impairments, quantization noise

Increasing the spectral efficiency of wireless communication systems has become more and more important due to the congestion of existing spectral resources. Motivated by this, several recent studies suggest that it is actually possible to receive and transmit data simultaneously with wireless radios using only one center frequency. These so-called full-duplex radios can potentially double the spectral efficiency, as they do not require separate frequency-bands for transmitted and received signals. However, all full-duplex radios experience strong interference from their transmitter chain, as the powerful transmit signal is coupled back to the receiver chain. This self-interference is the most significant obstacle when implementing a full-duplex radio in practice. Thus, an important feature for a full-duplex radio is the ability to attenuate its own transmit signal by some means.

This thesis investigates the effect of self-interference on the receiver chain of a practical full-duplex transceiver. It is assumed that the self-interference signal is attenuated both in the analog and digital domains, with two alternative techniques considered for the analog attenuation. Overall, information is provided regarding the magnitude of the different nonidealities occurring in the transceiver chain. The actual analysis is based on simplified models for the analog imperfections produced by the individual components. By utilizing these models, analytical expressions are derived for the power levels of the different signal components, and these power levels are then used to calculate the final achieved signal-to-interference-plus-noise ratio. Extensive numerical results are also provided with the derived expressions, using parameter values based on real transceiver implementations.

The obtained results demonstrate that a high number of bits is required in the analog-to-digital converter or, alternatively, that the self-interence signal must be significantly attenuated already in the analog domain. It is also shown that certain analog impairments, especially power amplifier nonlinearity, and possibly also the nonlinearity of the receiver components, must be addressed in digital self-interference cancellation. The reliability of the results obtained from the calculations is confirmed by their similarity with the results acquired from complete waveform simulations.

TIIVISTELMÄ

TAMPEREEN TEKNILLINEN YLIOPISTO
Signaalinkäsittelyn ja tietoliikennetekniikan koulutusohjelma
KORPI, DANI: Analogiset epäideaalisuudet langattomassa full-duplex lähetin/vastaanottimessa
Diplomityö, 65 sivua, 4 liitesivua
Helmikuu 2014
Pääaine: Langaton tietoliikenne
Ohjaajat: DI Taneli Riihonen ja TkT Lauri Anttila
Tarkastaja: Prof. Mikko Valkama
Avainsanat: full-duplex, epälineaarinen vääristymä, analogiset häiriöt, kvantisointikohina

Käytössä olevien taajuusalueiden ruuhkautumisen vuoksi langattoman tiedonsiirron spektritehokkuuden lisääminen on tullut yhä tärkeämmäksi. Vastauksena tähän, useat viimeaikaiset tutkimukset osoittavat, että on itseasiassa mahdollista lähettää ja vastaanottaa radiosignaaleja langattomasti käyttäen vain yhtä keskitaajuutta. Nämä niinkutsutut full-duplex lähetin/vastaanottimet voivat teoriassa jopa kaksinkertaistaa spektritehokkuuden, koska ne eivät tarvitse erillisiä taajuuskaistoja lähetetyille ja vastaanotetuille signaaleille. Haasteena tällaisessa tiedonsiirrossa on kuitenkin se, että lähetetty signaali on vastaanottimen näkökulmasta voimakas häiriölähde, sillä se kytkeytyy lähettimestä suoraan vastaanottimeen. Tämä itse-interferenssi on suurin käytännön este full-duplex lähetin/vastaanottimen toteutukselle, joten on erittäin tärkeää pystyä jollakin keinolla vaimentamaan sitä.

Tässä työssä tutkitaan itse-interferenssin vaikutusta tyypilliseen full-duplex lähetin/vastaanottimeen, kun itse-interferenssiä vaimennetaan sekä analogisesti että digitaalisesti. Lisäksi työssä esitetään analogiselle vaimennukselle kaksi vaihtoehtoista toteutustapaa. Kaiken kaikkiaan, työn tuloksena saadaan tietoa full-duplex lähetin/vastaanottimessa esiintyvien eri epäideaalisuuksien voimakkuuksista. Varsinainen analyysi perustuu yksinkertaistettuihin malleihin, joilla pyritään mallintamaan yksittäisten komponenttien synnyttämiä analogisia häiriöitä. Näiden mallien avulla johdetaan lausekkeet eri signaalikomponenttien tehoille, joilla saadaan laskettua lopullinen signaali-kohina-interferenssi suhde. Tämän lisäksi johdetuilla lausekkeilla lasketaan lukuisia esimerkkituloksia käyttäen todenmukaisia parametreja.

Saadut tulokset osoittavat, että analogia-digitaalimuunnoksessa vaaditaan runsaasti bittejä, tai vaihtoehtoisesti, että itse-interferenssiä täytyy vaimentaa analogisesti huomattava määrä. Lisäksi havaittiin, että tietyt analogiset häiriöt, etenkin tehovahvistimen aiheuttama epälineaarinen vääristymä, sekä mahdollisesti myös vastaanottimen epälineaarisuus, täytyy ottaa huomioon vaimennettaessa itse-interferenssiä digitaalisesti. Saadut tulokset ovat yhtäpitäviä aaltomuotosimulaatioilla saatujen tulosten kanssa, mikä vahvistaa niiden luotettavuuden.

PREFACE

This Master of Science thesis was written at the Department of Electronics and Communications Engineering at Tampere University of Technology in 2013.

Even though writing a thesis is always an individual effort, there are many people I must thank, and whose help deserves to be acknowledged. All the members of the full-duplex research group have provided invaluable insights into the general topic of this thesis, and thus have helped me to learn a lot. In addition, I would like to extend my gratitude to the whole digital transmission group for numerous inspiring lunch hour conversations and refreshing coffee breaks.

I must also most sincerely thank the supervisors of this thesis, M.Sc. Taneli Riihonen and D.Sc. Lauri Anttila, for sparing no effort in sharing their extensive knowledge regarding full-duplex communications, and also scientific writing in general. In particular, I would like to acknowledge the enormous amount of work Mr. Riihonen did in proofreading several drafts of this thesis. I feel that, in addition to greatly improving the final result of this project, his numerous comments and insights will also prove helpful in many future tasks and assignments.

Another important person for this thesis, and my work in general, has been Professor Mikko Valkama, who is the examiner of this thesis and also my supervisor at the Department of Electronics and Communications Engineering. I would like to thank him for giving me an opportunity to do scientific research in his group, as well as for inspiring the topic of this thesis. His expertise has been crucial in all of my research work.

Finally, I would like to acknowledge the love and support I have received from my family during the recent years, as well as during my whole life. Everything would have been impossible without it. Especially, and perhaps most importantly, I want to thank my lovely and dear wife, Eeva-Jonna. Her love has endured all the long evenings I have spent writing this thesis, and thus it has provided me with the most important of things: unwavering support in the face of every adversity and hardship as well as during each small victory. That has given me all the motivation I could have possibly needed, and even more. Thank you.

Tampere, February 2014

Dani Korpi

CONTENTS

ABBREVIATIONS AND NOTATIONS

ADC	Analog-to-digital converter
AGC	Automatic gain control
BPF	Band-pass filter
BS	Base station
DAC	Digital-to-analog converter
FD	Full-duplex
FDD	Frequency-division duplexing
LNA	Low-noise amplifier
LPF	Low-pass filter
MAC	Medium access control
MIMO	Multiple-input and multiple-output
MISO	Multiple-input and single-output
OFDM	Orthogonal frequency-division multiplexing
PA	Power amplifier
PAPR	Peak-to-average-power ratio
RF	Radio-frequency
QAM	Quadrature amplitude modulation
RX	Receiver
SI	Self-interference
SINR	Signal-to-interference-plus-noise ratio
SNR	Signal-to-noise ratio
SOI	Signal of interest
TDD	Time-division duplexing
TX	Transmitter
VGA	Variable gain amplifier
WLAN	Wireless local area network

1. INTRODUCTION

Wireless communications has been an important way of transferring information for a long time. Ever since from the times of telegraphs and AM-radio transmissions, to the modern era of cellular mobile networks, it has been an integral part of the human society. Nevertheless, due to the challenging nature of radio channels, only recently has there been a truly significant increase in the role of the wireless communications. The increased processing capacity of portable devices has allowed the development of smart phones and other highly mobile communications devices.

Nowadays, the ongoing research on wireless communications is constantly providing the consumers with faster and more reliable means of wireless data transfer. The growing demand for high data rates and low latencies in wireless communication methods has created a strong commercial interest in pushing the performance of wireless radios even further. Regardless of the immense amount of research already conducted in this field, there is still significant room for improvement in performance and efficiency. It is certain that only the laws of physics can halt the researchers' efforts to stretch the boundaries of wireless communication ever further.

However, the huge popularity of wireless communications has brought about also a significant problem. As wireless communications has become more and more widespread due to the possibility of constructing portable devices more cheaply, most of the usable frequencies are already in use by different systems. There are of course unlicensed frequency bands available but they are constantly congested because of them being used by so many different communications devices. This has created a strong motivation to develop techniques that enable the radios to use the available spectrum more efficiently.

Increasing the spectral efficiency is nowadays rather challenging because, due to the rapid development of wireless communications methods, the capacity of a single channel is in most systems already very close to the theoretical upper bound. Thus, it is not feasible to significantly increase the spectral efficiency of a single channel. For this reason, research has lately refocused on facilitating the co-existence of several data streams on one channel, as their combined spectral efficiency can still be improved in the form of spectrum reuse.

Related to this direction of research, it has recently been suggested that it is actually possible to receive and transmit data simultaneously with wireless radios

using only one frequency band. By employing such full-duplex radios, it is possible to potentially double the spectral efficiency, as there is no need for separate frequency-channels for transmitted and received signals. Furthermore, since transmission and reception happen at the same time at the same center frequency, the transceivers can sense each other's transmissions and react to them. This, with appropriate medium access control (MAC) design, can result in a low level of signaling and low latency in the networks. In fact, because of these benefits, full-duplex radios may revolutionize the design of radio communication networks.

One of the most interesting benefits of full-duplex radios is perhaps their ability to avoid the hidden node problem [20, 50]. It is made possible by the simultaneous transmission and reception, as each communicating full-duplex radio thus reserves the medium and prevents potential collisions. Solving the hidden node problem in this manner can increase the fairness and throughput for example in networks utilizing carrier-sense multiple access based techniques.

Full-duplex radios might also be utilized in cognitive radio networks, where they could potentially provide large system performance gains. The reason for this lies, again, in their ability to transmit and receive signals simultaneously on a single center-frequency. With this ability, secondary users could constantly monitor the spectrum for primary users, and thus avoid any overlap with their and primary users' spectrum usage. Hence, as avoiding the collisions between the primary and secondary users' signals is one of the main problems in cognitive radio technologies, the role of full-duplex radios might prove to be crucial in this context.

1.1 Research problem

The most significant obstacle in implementing a functional full-duplex radio is the problem of *self-interference* (SI). It results from the fact that the transmitted signal is superposed with the received signal of interest, and as they share the same frequency band, it usually cannot be filtered out. Thus, one of the central problems in studying full-duplex radios is to determine ways to cancel the SI signal down to a sufficienly low level. However, due to several inherent non-idealities in the implementation of SI cancellation stages, e.g., phase mismatch in the cancellation signals and the nonlineary of the amplifiers, there will always be some residual SI after them.

In this thesis, the goal is to study the effect of transceiver component nonlinearities on the performance of full-duplex transceivers, and especially on the achievable realistic SI cancellation. Nonlinearity is an especially interesting problem in full-duplex radios since, compared to a conventional half-duplex receiver, the operation region of the receiver components must also handle the high-power SI signal, because it does not go through the final suppression until after analog-to-digital conversion.

The linearity requirements for different electronics components may therefore be much stricter than in conventional transceivers, which is not fully analyzed or understood in the earlier literature and experiments of the full-duplex field.

Furthermore, in addition to receiver chain characteristics, the linearity of the transmitter chain is also a key factor in designing full-duplex transceivers. Namely, the nonlinear distortion induced by the power amplifier (PA) of the transmitter may be a significant factor also at the receiver, since the available solutions for SI cancellation rely on linear signal processing models. Thus, the effect of the nonlinearity of the transmitter chain should be analyzed as well and taken into account when studying the feasibility of single-channel, full-duplex communications.

Another issue, which will be studied in detail in this thesis, is the dynamic range of the receiver chain's analog-to-digital converters (ADCs). If there is a need to further attenuate the SI in the digital domain, additional dynamic range is needed as the powerful SI signal will effectively decrease the resolution of the desired signal.

As elaborated later, the possible applications for full-duplex radios are numerous. The knowledge of the usefulness of full-duplex radios provides strong motivation to study them further, and solve the remaining implementational problems. For this reason, this thesis expands the knowledge about practical full-duplex transceivers, and by these means advances their advent to commercial usage.

1.2 Contributions

The contributions of this thesis are as follows.

- This thesis derives an analytical model for a complete direct-conversion full-duplex transceiver, including both analog and digital self-interference cancellation stages. The model takes into account also the effects of the different analog imperfections, and it can be used to determine the power levels of the different signal components at the detector input of a full-duplex transceiver, using arbitrary parameters.

- The required ADC dynamic range and resolution requirements are explicitly derived such that the signal-to-interference-plus-noise ratio (SINR) in the receiver chain will not degrade more than a specified implementation margin allows.

- Continuing from the above, this thesis derives an equation for the effective amount of lost bits due to the self-interference signal, which can be used to obtain additional insight into the requirements for the ADC.

- It is shown especially that, with typical parameters, the PA-induced nonlinearities can cause significant distortion at the detector already with typical transmit powers, e.g., in WiFi or cellular devices.

- Furthermore, it is shown that attenuating the nonlinearly distorted component of the SI signal will provide performance gain for full-duplex transceivers. Taking also into account the observation about the strength of the PA-induced nonlinear distortion, this thesis illustrates the clear need for nonlinear self-interference cancellation mechanisms.

- One tangible outcome of this thesis is a full waveform simulator capable of modelling several aspects of practical full-duplex transceivers on signal level. Although this simulator is used herein mainly to confirm the reliability of the analytical models, it will be an useful tool in the future work on this topic.

In addition, a journal article has been written based on the results obtained in this thesis [39]. This article is currently under peer-review. The results of this thesis were also utilized in another scientific article, which has already been published [40].

1.3 Outline

The rest of this thesis is organized as follows. In Section 2, the past and current research on full-duplex communication is briefly overviewed. This is done in order to justify the topics of this thesis, and to show that a research gap exists. After that, in Section 3, the model of the analyzed full-duplex transceiver is presented. Here, the structure of the transceiver is discussed in detail, and the properties related to full-duplex operation are thoroughly explained. Section 4 presents the principles of the system calculations used to analyze the full-duplex transceiver. The essential equations, including those describing the actual signal models, are also presented and discussed. Then, Section 5 presents the main results of the system calculations, and discusses the most relevant findings. The calculations are done for two different architectures, and with two different sets of parameters. After that, in Section 6, the results of the analytical system calculations are verified by comparing them to the results of complete waveform simulations. The waveform simulator is also briefly discussed. Finally, conclusions are drawn in Section 7.

1.4 Nomenclature

Throughout the thesis, the usage of linear power units is indicated by lowercase letters. Correspondingly, when referring to logarithmic power units, uppercase letters will be used. The only exception to this is the noise factor, which is denoted by capital F according to common convention in the literature of the field. Watts (W) are used as the absolute power unit and decibels per milliwatt (dBm) as the logarithmic power unit.

2. SINGLE-CHANNEL FULL-DUPLEX COMMUNICATION

The pioneering work in the theory of communications was done by Claude E. Shannon already in the late 1940s. In [65], Shannon derives the maximum capacity of a communication channel. This limit is known as the Shannon–Hartley theorem. It describes the maximum transfer rate achievable on a noisy channel. Let us mark the power of the signal of interest by p_{SOI} and the power of the noise by p_{N}. Now, if the signal-to-noise-ratio is denoted by $SNR = \frac{p_{\mathrm{SOI}}}{p_{\mathrm{N}}}$ and the channel bandwidth is W, the maximum transfer rate of the corresponding communication channel in bits per second is given by

$$C_{\max} = W\log_2(1 + SNR) = W\log_2\left(1 + \frac{p_{\mathrm{SOI}}}{p_{\mathrm{N}}}\right) \tag{2.1}$$

This equation assumes that the noise has a Gaussian distribution and that Gaussian codewords are used when coding the signal of interest. Especially the latter assumption is usually quite unrealistic but, nevertheless, (2.1) illustrates what is required to achieve a certain data rate. Thus, even if the capacity given by (2.1) is somewhat optimistic, it still shows the relation between SNR, bandwidth, and data rate.

Nowadays, by utilizing modern adaptive modulation and adaptive coding methods, it is possible to get relatively close to the maximum capacity of a given bandwidth even with practical systems. However, an important observation from (2.1) is that the capacity is also limited by the bandwidth of the channel, in addition to the SNR. This is perhaps one of the main reasons for the scarcity of the spectral resources, as more and more bandwidth is reserved by different systems to increase their data rates. Due to the capacity limit given by (2.1), there has been no other feasible way to respond to the increasing demands for mobile data transfer. However, as mentioned, full-duplex transceivers are one possible answer to this problem, as they provide a significant increase in spectral efficiency.

There are still several problems to be solved in practical realization and implementation of small and low-cost full-duplex transceivers, but many promising results have already been achieved with this technology. One of the issues is that, in this type of full-duplex radio, the transmitted and received signals interfere with each other freely as there is no means to separate them [16]. This produces self-caused

interference, or self-interference (SI), which must be attenuated by some means. In essence, SI results from the fact that in a full-duplex radio, the transmitter and receiver use either the same [23, 37] or closely separated antennas [20, 27, 31, 62]. Therefore, the receiver chain of the transceiver receives the transmitted signal from its own transmitter chain. In wireless communications, this creates severe problems in the receiver front-end of such a full-duplex link, because the signal of interest, propagating in the air from a distant transmitter, is strongly attenuated, and it is thus very weak once it reaches the receive antenna. In fact, simple link-budget calculations reveal that the SI signal can be in the order of 60-100 dB (depending on implementation, e.g., on antenna separation) stronger than the received signal of interest, especially when operating close to the sensitivity level of the receiver chain.

Thus, in order to achieve high levels of spectral efficiency with a full-duplex radio, large amounts of SI must be cancelled. In principle, the SI signal is perfectly known at the receiver since the transmit data is known inside the device. That is why, again in principle, the SI can potentially be removed perfectly from the received signal because the basic idea in cancelling SI is subtracting the known transmitted signal from the overall received signal. This must be done already at the RF front-end in order to prevent the saturation of certain components. In the analog domain, the subtraction can be done by adding a properly delayed and attenuated version of the transmitted signal with a phase difference of 180 degrees to the received signal, which should ideally cancel all of the SI, assuming a sufficiently narrow bandwidth. However, because the SI signal propagates through an unknown channel linking the transmit (TX) and receive (RX) paths, and is also affected by unknown nonlinear effects of the transceiver components, having perfect cancellation is, in practice, far from realistic. The SI can be further mitigated digitally after the signal has been sampled. Now the transmitted samples must be filtered and subtracted from the received samples in order to reduce the effect of self-interference. When these two methods are combined, it is possible to attenuate the SI signal to a sustainable level.

With (2.1) it is possible to also determine the maximum transfer rate of a full-duplex communication channel, denoted by $C_{\mathrm{max,FD}}$. Since the received and transmitted signals utilize the same center-frequency, $C_{\mathrm{max,FD}}$ consists of the maximum transfer rate of both the transmit and receive channels. In practice, these indicate the maximum rates with which two full-duplex transceivers can receive simultaneously data from each other. To take also the nonidealities of the full-duplex transceivers into account, it is assumed that there is some residual SI after SI cancellation, denoted by $p_{\mathrm{SI,resid.}}$. Now, assuming that both full-duplex transceivers operate under similar conditions and have similar SI cancellation capabilities, i.e., they can achieve the same signal-to-interference-plus-noise ratio (SINR), the maxi-

mum transfer rate can be written as

$$\begin{aligned} C_{\mathrm{max,FD}} &= C_{\mathrm{max,rx}} + C_{\mathrm{max,tx}} \\ &= W\log_2(1 + SINR_{\mathrm{FD}}) + W\log_2(1 + SINR_{\mathrm{FD}}) \\ &= 2W\log_2\left(1 + \frac{p_{\mathrm{SOI}}}{p_{\mathrm{N}} + p_{\mathrm{SI,resid.}}}\right) \end{aligned} \tag{2.2}$$

As mentioned earlier, this equation assumes that the noise and residual SI signals follow a Gaussian distribution. In some cases, this requirement might not be fulfilled, and the actual maximum capacity might differ from the value predicted by (2.2). Nevertheless, (2.2) still provides a feasible approximation for the theoretical maximum capacity of a full-duplex radio.

If it is assumed that the SI cancellation performance of the full-duplex transceivers is very good, it can be written that $p_{\mathrm{SI,resid.}} \approx 0$, and the maximum transfer rate becomes

$$C_{\mathrm{max,FD}} \approx 2W\log_2\left(1 + \frac{p_{\mathrm{SOI}}}{p_{\mathrm{N}}}\right) \tag{2.3}$$

which is two times the transfer rate of a traditional half-duplex system. Thus, it can be observed that with sufficient SI cancellation ability, significant performance gains can be achieved by single channel full-duplex communication. Furthermore, as no additional bandwidth is required, also the spectral efficiency of full-duplex transceiver is doubled compared to a half-duplex radio. This is perhaps the most significant asset of single channel full-duplex communication. It must be noted, however, that the doubling of the spectral efficiency occurs only when both of the two parties have data to transmit. Otherwise, there is obviously no gain in being able to transmit and receive data simultaneously.

2.1 Full-duplex transceiver types

Most of the research on single channel full-duplex communications has focused on relay applications in the past. This is understandable, as in relays it is desirable to utilize only the available resources and retransmit the received signal on the same frequency band. However, lately the research has focused more towards a general full-duplex radio. The reason for this is perhaps the desire to utilize even more widely the several benefits of simultaneous transmission and reception on a single frequency band. It is also worth noting that a general full-duplex radio can also be used as a relay.

2.1.1 Full-duplex relay

A relay is a device that receives a signal, possibly decodes it, amplifies it, and transmits the amplified version of the signal. It is desirable to do this using only one frequency band, as in such a case no additional spectral resources are required by the relay [55, 57]. However, if the original transmission is continuous, it is not possible for a traditional half-duplex relay to retransmit the signal, as that requires time gaps in the original transmission. Thus, if the relay is implemented with half-duplex radios, relaying requires additional resources, either in time or frequency domain.

For the above reason, in the relaying context, single-channel full-duplex radios provide significant benefits compared to traditional half-duplex solutions. No additional resources are required, as the received signal can be transmitted again on the same frequency band [25, 55, 57]. Furthermore, the delay introduced by the relay is very small, as it consists only of the processing delay occurring inside it.

The requirements for a full-duplex relay are largely similar to those of a general-purpose full-duplex transceiver. The SI signal must be attenuated by a certain amount for the relay to provide a sufficient SINR for the relayed signal. The SI cancellation on full-duplex relays has been widely studied. For example, in [58] a very thorough analysis is carried out regarding the realistically achievable SI suppression.

However, unlike in a general full-duplex transceiver, more isolation can be provided for the transmit and receive antennas, as they do not have to be physically in the same location [32]. The antennas can, for example, be separated on the opposite sides of the outer wall of a building. This will provide a significant amount of attenuaton for the SI signal due to the increased propagation loss between the antennas, and hence the SI cancellation requirements are somewhat smaller than for a general full-duplex radio.

In addition to spatial separation, a proper weighting of the transmitted and received signals of the relay can significantly attenuate the SI power. This has been analyzed in [22], [35], and [44]. In [35], the authors consider a situation where, in addition to the actual relay, also the original transmitter and the final receiver weight the signal using their own weighting matrices. By choosing the weights correctly, this kind of processing can increase the final SINR. In [44], only relay weighting is considered, but with the objective of maximizing the ratio between the signal of interest and the SI signal, instead of only nulling the self-interference. In [22], weighting inside the relay is considered, but now the processing matrix is calculated over continuous domain, instead of the more usual digital domain.

In the full-duplex relaying context, also the optimization of the transmit power is an important topic, as it directly determines the power of the self-interference. However, the transmit power cannot be set too low, as that would decrease the SINR

of the final receiver too low, so selecting the transmit power of a full-duplex relay is always a trade-off. This topic is studied in [67], where a distributed transmit power algorithm is presented for full-duplex relays. The presented algorithm is a practical method for determining the transmit power, as no control channel is required. The transmit power allocation is also analyzed in [36], where the optimal transmit power for minimizing the outage probability in a cognitive radio network is determined. In addition, transmit power adaptation is studied extensively in [57] and [56]. There, several different gain adaptation algorithms are analyzed in terms of maximizing the SINR under residual SI.

In addition to these studies, also other methods have been suggested for minimizing the effect of self-interference. In [69], the authors study an OFDM full-duplex relay, and concentrate on minimizing inter-symbol and inter-carrier interference when attenuating the SI signal. In [43], a distributed beamforming solution for full-duplex relays is proposed, where each mobile and relay station performs transmit beamforming and receive combining to suppress SI at the relay. Furthermore, the proposed method allows to do this in an iterative manner, and without any additional information exchange between the nodes.

In addition to transmit beamforming, also the steering of the receive array has been studied. In [11], the authors present an adaptive SI canceller for MISO full-duplex relays, which, among other methods, steers the receive array towards the most distortionless response. The proposed canceller performs also temporal filtering to attenuate the SI signal.

Similar to general full-duplex transceiver, the dynamic range of the ADC is a concern also in the relay context. In [25], a full-duplex relay under limited dynamic range is analyzed. The analysis discusses and studies the decrease in the resolution of the signal of interest, caused by the strong SI signal. Especially, the achievable rate under limited dynamic range is calculated.

A more general approach to full-duplex relaying was taken in [54], where the tuning of the phase of the signal within the relay is analyzed. It is shown that this type of a technique will result in coherent combining of the original and relayed signals at the final destination, and thus increase the achievable rate.

Overall, it is evident that full-duplex relays would provide significant performance gains over the traditional half-duplex based relays. Furthermore, as the full-duplex relays have less stringent SI cancellation requirements due to the possibility of a large separation between the transmit and receive antennas, relaying is certainly a potential application for the first commercial full-duplex transceivers. Nevertheless, the ultimate objective is still to be able to construct a compact device that is capable of single-channel full-duplex communication under all types of circumstances.

2.1.2 General full-duplex transceiver

In this thesis, a general full-duplex transceiver is considered, as this allows for the results to be applied to most of the full-duplex communications scenarios. This is also where the scope of the research has shifted in the recent years. Thus, the achieved results apply to all full-duplex transceivers, including relays. For this reason, the point of view of the analysis of this thesis is well justified.

One of the first practical demonstrations of a full-duplex radio is done in [17]. There it is shown that it is possible to significantly attenuate the SI coming from the transmit antenna when using only one frequency band for both transmission and reception. A similar type of practical analysis is carried out more recently in [20, 27, 31, 50]. These studies indicate that the idea of simultaneous transmission and reception on a single frequency band is feasible also in practice. However, the implementations still have severe limitations, which include insufficient amount of SI cancellation, low bandwidth, and non-idealities occurring in the transceiver chain. Further research is required in order to solve these problems and extend the operation range of the current full-duplex radios.

In terms of the antenna structure, perhaps the most intuitive approach is to use two antennas; one for reception and one for transmission. This is the most widely used antenna solution for the implemented general full-duplex radios [17, 27, 31, 50]. However, also other solutions have been used, including the three-antenna implementation in [20]. There, two antennas were used for transmission, and the receive antenna was positioned to the null between the two transmit antennas. This provided additional attenuation for the SI signal. Another interesting option is to use only one antenna. This is studied, e.g., in [37], where circulators are used to divide the antenna between the transmitter and the receiver. It is shown that the circulators attenuate the SI signal by a similar amount as when using separate antennas. There have also been other successful implementations of a full-duplex transceiver using only one antenna [23, 48]. These studies provide promising results in terms of implementing a mobile full-duplex radio, as it is desirable to use only one antenna in this context.

An experimental study on the active SI cancellation ability of a full-duplex radio is carried out in [26]. There, several characteristics regarding the achieved SI cancellation are revealed and analyzed with the help of measurements. Other studies concentrating on SI cancellation in general full-duplex radios include [34] and [45]. In the latter, a novel and improved method for analog SI cancellation is demonstrated. Unlike in the traditional approach, with the proposed method also the multipath components of the SI signal can be attenuated, resulting in an increased amount of cancellation in the analog domain. In the former, a method for wideband digital cancellation is presented, and it is shown that with the proposed method, a higher

amount of digital cancellation can be achieved for wideband signals. In [53], spatial domain suppression and time domain cancellation are compared in the context of a bidirectional full-duplex MIMO link. Large-system analysis is then performed to characterize the rate loss of suppression versus cancellation, and in particular, the effect of allocating some of the spatial degrees of freedom for SI suppression. Spatial domain suppression is also studied in [64], where also the effect of quantization noise is included in the modeling. It is observed that, due to hardware limitations, spatial suppression in itself is not sufficient to attenuate the SI below the noise floor.

In order to understand better the non-idealities and problems of the practical implementations, also theoretical research and simulations studies have been performed on general full-duplex radios. A basic study, based on full-duplex transceiver simulations, is performed, for example, in [42]. Another theoretical study was carried out in [46], where also a MAC for full-duplex radio is proposed and simulated, in addition to the analysis of the actual full-duplex transceiver. An optimal power allocation scheme for full-duplex radios under a given QoS constraint is presented in [19]. The scheme is derived for two situations: one where the power of self-interference is related to the transmit power, and one where it is not. In [38], the effect of IQ imbalance in full-duplex transceivers is analyzed. The authors also propose a novel digital cancellation scheme for attenuating the conjugate SI caused by the IQ imbalance and verify its performance with simulations.

Analyses on the effect of transmit imperfections in full-duplex radios in cognitive radio context are carried out in [24, 25, 58, 73]. There, it is analyzed how the residual SI resulting from the non-idealities in the transmitter chain affects the performance of the transceiver. However, in these studies the modelling of the transmit imperfections is very simplified, and the need for a more detailed analysis still exists.

Recently, the effect of nonlinear distortion in a general full-duplex transceiver, and its compensation, have also been studied, e.g., in [8, 12, 15, 41]. These studies indicate that nonlinear distortion of transceiver components, in particular with low-cost mass-product integrated circuits, forms a significant bottleneck for practical full-duplex radio devices. The findings of this thesis support also the conclusions made in these studies, and provide further motivation for nonlinear SI cancellation.

Several recent studies have also analyzed the phase noise of the transceiver oscillators [9, 52, 61, 68]. In these studies it is observed that the phase noise can potentially limit the amount of achievable SI suppression, especially when using separate oscillators for transmitter and receiver. The effect of phase noise is also considered in [63], where the feasibility of asynchronous full-duplex communications is studied. Although it is evident that also oscillator phase noise can represent a performance bound in FD devices, the focus in this thesis is on nonlinear distortion and ADC interface, and thus phase noise is neglected in the analysis.

2.2 Applications for full-duplex transceivers

In addition to providing increased data rate and spectral efficiency, full-duplex radios can be used in several new applications which utilize their ability to transmit and receive simultaneously on the same frequency band.

2.2.1 Efficient data transfer

The most obvious benefit of a full-duplex transceiver is the ability to transmit while receiving data, which in some cases doubles the observed data rate. However, this requires that there are two FD-capable transceivers, both of which have data to transmit to each other. Nevertheless, if it is assumed that there is a sufficient amount of data travelling to both directions, the increase in the data rate caused by full-duplex communications is significant.

Theoretically, the maximum capacity is defined by (2.2), and it can be observed that it is dependent on the power of the residual self-interference. Thus, if it is accepted that there is always some residual SI, the maximum capacity of the channel is not quite doubled. However, it has been shown in several publications that a significant increase in the measured data rate is still achieved [15, 20, 31, 62]. This also justifies the increased complexity required to cancel the SI signal, since lots of gain in terms of the data rate is achieved.

2.2.2 Full-duplex base station

One possibly advantageous use case for a full-duplex transceiver would be to utilize it in the base station (BS) of a cellular network [28]. The reason for this is that, in mobile communications, it would be sensible to include as much of the complexity as possible in the base station. This would allow the mobile users to have cheaper and less complex equipment, decreasing the overall cost of the network. Hence, one possible way to utilize this principle would be to make only the base station full-duplex capable.

A full-duplex base station could serve two mobile users at the same time, without requiring any additional spectral or temporal resources. This, of course, requires sufficient spatial separation between the mobile users to minimize the interference caused by the transmitting uplink mobile user to the receiving one in downlink direction. Also, unlike two full-duplex transceivers communicating with each other, the base station is more likely to have data to transmit and receive at any given time, as it is serving several users at once. This would allow it to utilize the additional capacity provided by the full-duplex capability in a very efficient manner, possibly even achieving the doubling of the data rate at busier hours.

However, in this type of a network, where only the BS is full-duplex capable, there are certain problems. One obvious issue is that if there is only one terminal in the network, the full-duplex capability of the BS will be of no use. In this case, the BS and terminal must communicate in half-duplex mode. This indicates that full-duplex base stations should not be utilized in rural areas, where the density of the mobile users is not sufficiently high. For the same reason, it might not be beneficial to utilize full-duplex base stations in the so-called femtocells, which are likely to serve also very few users at a time [4].

Moreover, if the terminals do not have strict traffic requirements and the BS subsequently has no need to transmit and receive simultaneously, the gain of the full-duplex BS compared to a half-duplex BS is small. However, it is likely that there are times when the traffic load is higher and in such a case the FD capability will bring capacity gain. But if there is little traffic and it is divided unevenly between up- and downlink, a half-duplex system is likely to perform equally well as a full-duplex system. This is due to the fact that a full-duplex system is most efficient when there is equal amount of data to be transmitted and received.

Another challenging situation is when all the terminals are located too close to each other. In this case they cannot communicate simultaneously with the BS because one terminal transmitting while another is receiving would cause too much interference [60]. This interference differs from self-interference in the sense that it is not known by the receiving node, and hence it is very challenging to compensate for it. Thus, also in this case the network is forced to operate only in half-duplex mode. However, it is easy to avoid this type of a situation by choosing the boundaries of each cell so that the BS is approximately in the middle of the mobile users. By choosing the simultaneously served mobile users from different sides of the cell, the amount of interference between them can be minimized.

Depending on the implementation of the full-duplex base station, there might also be some special limitations that must be taken into account. In [62], Sahai et al. observe that, when considering a random access network, it is not possible to start a new transmission during an ongoing reception. The reason for this is that it is then impossible to estimate the self-interference channel without losing a part of the received signal. Thus, since both analog and digital self-interference cancellation require some knowledge about the channel, it is clear that this limitation must be taken into account when designing a network based on full-duplex base stations.

2.2.3 MAC-level benefits

In addition to increased data rate, also some benefits in the medium access control (MAC) level can be achieved when using full-duplex transceivers [20,31,50,62]. The most significant issue, which can be solved relatively easily when using full-duplex

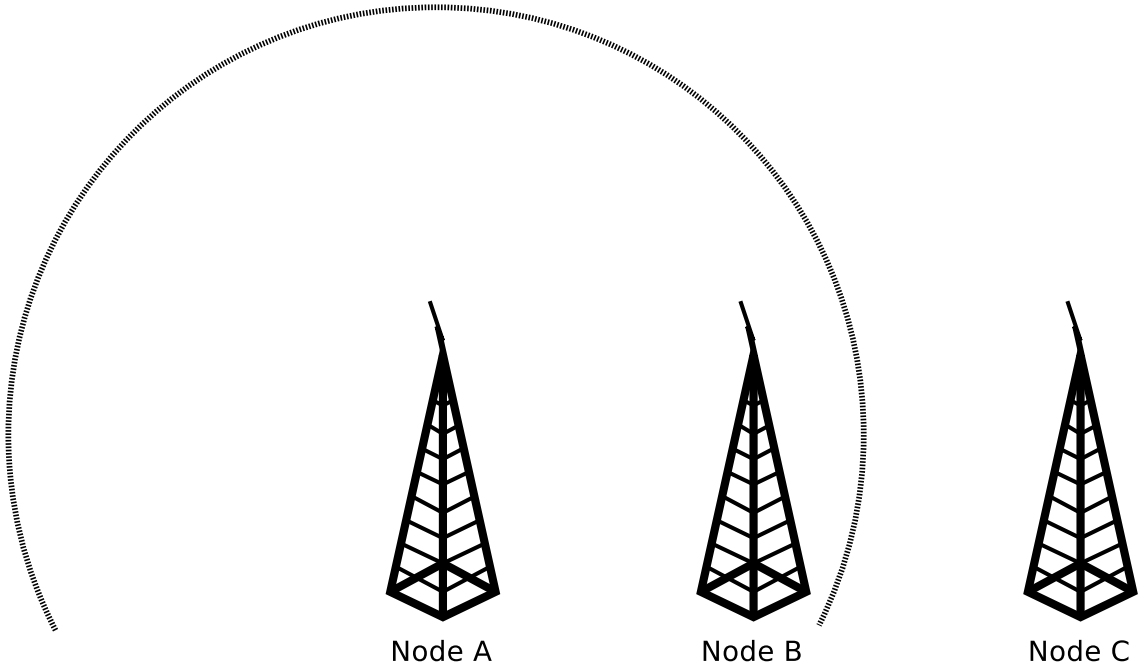

Figure 2.1: An illustration of the hidden terminal problem. The gray line depicts the transmissions from Node A. Node C is unable to hear this transmission, and it might also try to send a packet to Node B, causing a collision.

transceivers, is the hidden node problem, a persistent issue in carrier sense multiple-access networks. Figure 2.1 illustrates a typical situation in a wireless network, where three nodes (A, B, and C) are communicating. If Node B is an access point or a base station, both nodes A and C are likely to have data to transmit to it most of the time. In this kind of a situation, if Nodes A and B are outside each others' hearing range, they cannot sense the medium being busy if the other one is transmitting a packet, and may try to transmit simultaneously a packet to Node B. This, on the other hand, means that the packets will collide, and must be retransmitted.

If the nodes are full-duplex capable, however, this situation is significantly less probable to happen. In such a scenario, also the receiving node is able to transmit simultaneously. Thus, in the example of Fig. 2.1, Node B is also transmitting a packet while it is receiving one from Node A. This means that Node C will sense the medium as busy and will not try to transmit anything. Due to less collisions because of the simultaneous transmission and reception, the overall throughput of the network will increase [20]. Thus, full-duplex capable transceivers will also increase the performance of a network through MAC level benefits.

In addition to solving the hidden node problem, using full-duplex transceivers has also been shown to increase the fairness in a network. In [31], it was observed that in a typical half-duplex network where the same access point is shared by several nodes, the transmissions of the access point were heavily congested. The reason for

this is that it has obviously the most packets to transmit, as it is serving several nodes, but it might not be able to reserve the medium often enough to transmit them efficiently. However, if the access point and the nodes are full-duplex capable, this is not a problem, as the access point can always transmit a packet to the node that it is receiving from. Assuming sufficiently symmetrical traffic patterns, this will significantly increase the fairness of the network [31].

2.2.4 Cognitive radio

Perhaps one of the most interesting uses for the ability to transmit and receive simultaneously on the same frequency band is found in the cognitive radio networks. One of the most significant challenges in implementing a feasible cognitive radio is to be able to detect and avoid blocking a primary transmission [10]. With a traditional time-division duplexing (TDD) system, this must be done between certain intervals by ceasing the own transmission, and listening to the channel for primary transmissions. However, there are two problems with this approach. Firstly, the overall efficiency is not very good, as there must be gaps in the channel usage to listen for primary transmissions. Secondly, if the primary transmission occurs between these listening gaps, a collision will occur, and this will also decrease the data rate of the primary user.

To combat these issues, full-duplex radios have been suggested, e.g., in [20], to be used in cognitive radio applications. Since it would be possible to both transmit and receive simultaneously with a full-duplex radio, there would be no need for specific listening gaps, as the receiver chain could be used to monitor the spectrum continuously while transmitting. In other words, during transmission, the receiver chain would be used to sense the spectrum instead of receiving actual data signals. This would significantly decrease the performance loss of the primary users, as their transmissions would be detected in real-time, and collisions would be thus avoided.

However, similar to other applications for full-duplex radios, the feasibility of this particular application depends on the SI cancellation ability of the full-duplex radio. If the power of residual self-interference after all the cancellation stages is still high, the detection probability of primary transmissions might be relatively low. This, on the other hand, would render the benefits of the full-duplex radio useless. However, as there is no need to decode the detected transmissions, the SI cancellation requirements in cognitive radio context are not as high as in ordinary transceiver applications.

There has been some research also on this special topic. For example, in [18], the benefits of full-duplex spectrum sensing are theoretically analyzed. It is also shown that throughput is higher for both the primary and secondary users when using the proposed full-duplex spectrum sensing scheme, in comparison to half-

duplex spectrum sensing. Similar type of results are obtained in [6], where it is also shown that rate gains can be achieved with simultaneous transmission and sensing in cognitive radio networks. In addition to comparison between half-duplex and full-duplex spectrum sensing, also different antenna configurations are compared in [6]. It is shown that in order to benefit from full-duplex operation, a certain type of antenna configuration should be used. In [73], a cognitive radio base station is analyzed under the assumption that it operates in full-duplex mode, but under residual SI. Different algorithms are provided to maximize the rate of the cognitive radio system.

2.2.5 Security applications

There have also been some suggestions on how to improve the security of wireless data transfer with full-duplex communications [71, 72]. These methods rely on the fact that it is challenging to correctly detect the superposed waveform of two transmitted signals without prior knowledge of their structures. Thus, by transmitting a jamming signal simultaneously while receiving, eavesdropping of the received signal is made very challenging. For the recipient of the transmission, decoding the message is possible as it obviously knows its own transmission signal and can cancel it out from the received signal. However, for anyone else, it is nearly impossible to decode the signal. This obviously increases the security of data transfer, as long as both parties transmit a signal.

Transmitting a jamming signal while receiving a signal on the same channel is studied in [71]. They utilize a similar antenna cancellation scheme that was presented in [20] to attenuate the self-interference signal before the actual reception. A significant increase in the network secrecy is reported when using this method. An important observation is that the jamming signal must have an unknown structure, or no structure at all, to increase the security. Namely, in [30] it is shown that two collided packets can be successfully decoded under certain conditions, assuming that their general structure is known. Thus, transmitting a jamming signal of known structure will not likely prevent eavesdropping.

A more general study is performed in [72], where the authors analyze the secrecy when the destination is a MIMO full-duplex transceiver. Also here, the destination is assumed to transmit a jamming signal in addition to receiving the actual information signal. It is shown that under both perfect and imperfect channel state information, the full-duplex capability of the destination node allows for a significant improvement in the secrecy rate. Thus, if secrecy is preferred over high data rate, a full-duplex transceiver can also be used to improve the secrecy of data transfer, instead of only improving the data rate.

2.3 Selection between full-duplex and half-duplex

As full-duplex transceivers typically require at least one transmitter and one receiver chain, as well as two antennas, it is natural to compare a single-channel full-duplex transceiver to a half-duplex MIMO transceiver that has the same resources available. In theory, both solutions should achieve the same overall throughput when two transceivers are communicating. However, in [31] it is observed that with higher SNR, better throughput is achieved with two full-duplex transceivers, whereas with lower SNR, the data rate is higher with two half-duplex 2x2 MIMO transceivers. This indicates that it might be beneficial to implement transceivers capable of both MIMO and full-duplex communications, depending on the channel conditions.

In [13], the authors discuss the problem of choosing between MIMO and full-duplex operating modes. They propose that in order to achieve the highest possible throughput, the device should be capable of both. Thus, a full-duplex radio capable of also MIMO communication is implemented, and compared against a traditional MIMO system. It is shown that the full-duplex/MIMO capable radio outperforms the radio capable of only MIMO operation. Similar results are obtained in [5], where it is observed that with the same amount of RF chains, a MIMO system performs better in the low SNR region, and a full-duplex system achieves better throughput with higher SNRs. In [66], the comparison between MIMO and full-duplex is done for relays. There it is also shown that under certain SNR regions, MIMO will provide higher data rate, whereas in the other regions full-duplex is the better option. In [55] and [57], the performance of half-duplex and full-duplex systems is also compared in the relaying context, and it is shown that with practical SNR values, it is preferable to use a full-duplex relay rather than a half-duplex relay.

Full-duplex and half-duplex modes are also briefly compared in [7]. The authors observed that, with lower transmit powers, using full-duplex operation provided higher data rate. With higher transmit powers, on the other hand, half-duplex mode outperformed full-duplex mode. This is shown to be due to the increased power of residual SI caused by insufficient cancellation. With higher transmit powers, the SINR became too low because of higher self-interference power, and this resulted in the decreased performance of the transceiver utilizing full-duplex communication.

Overall, it is thus evident that it would be desirable to implement such a full-duplex transceiver that is also capable of half-duplex MIMO communications [5, 13, 31]. This would allow it to achieve higher average data rate when the SNR varies significantly. However, it must first be determined how a full-duplex transceiver can be implemented in an efficient and feasible manner. After that, the next step is to determine whether it is possible to construct a transceiver in such a way that it includes also the necessary components for MIMO architecture.

2.4 Effect of non-idealities on self-interference cancellation

As already discussed, the most significant issue in implementing a feasible full-duplex transceiver is the residual self-interference left after all cancellation stages. In this thesis, three stages of SI attenuation are assumed, namely the isolation between the antennas (antenna attenuation), active cancellation in the analog domain (RF cancellation), and active cancellation in the digital domain (digital cancellation). If the level of this residual SI is too high after these cancellation stages, the performance of the full-duplex transceiver might be even lower than that of a traditional half-duplex system. Thus, it is crucial that a sufficient amount of SI is cancelled before the detection stage. However, this requires a deeper understanding of all the non-idealities occurring within full-duplex transceivers, as these nonidealities are often limiting the achievable SI cancellation. Of course, in many cases the actual SI cancellation method might not be optimally precise (e.g., due to imprecise SI channel estimation), but at some point the nonidealities become a limiting factor for the maximum achievable cancellation and thus prevent the transceiver from achieving the desired data rate.

2.4.1 Antenna attenuation

There are various limitations for the performance of the SI cancellation stages. The antenna attenuation is obviously limited by the distance between the transmit and receive antennas, as well as by their orientation and beam pattern. In some applications, especially in the relaying context, it might also be possible to position the antennas in such a manner that there is something physical between them, for example, the device itself. This will obviously increase the amount of antenna attenuation due to increased path loss [62]. However, the amount of antenna attenuation does not depend on the non-idealities occurring in the transceiver chain, obviously.

2.4.2 RF cancellation

The performance of RF cancellation is limited by several factors. Perhaps the most significant one is the quality of the RF circuitry used in implementing the cancellation [20, 31]. The most critical operation is obtaining an inverse of the transmitted signal and then attenuating and delaying it properly to match the actual SI signal. It has been observed in literature that the accuracy of the delay is in many cases the bottleneck in RF cancellation, especially for wideband signals [31].

Another limit for the performance of RF cancellation is also the quality of the SI channel estimate. Actually, knowledge of the attenuation and delay of only the main signal component is sufficient in most cases, as the direct signal path is obviously the most powerful one [20, 26, 31]. Thus, enough RF cancellation can be achieved

by attenuating only this signal path. This also decreases the complexity of the RF circuitry, as attenuating the multipath components would require additional cancellation signal paths and a more complex channel estimation procedure.

However, in [15] and [21], a different type of RF cancellation procedure is proposed. The reported implementation uses several fixed delay lines for the reference signal, each of which has a tunable attenuator. Essentially, the cancellation signal is filtered with an analog FIR filter. The objective is to generate a more precise copy of the direct self-interference component by using a linear combination of slightly delayed versions of the reference signal. In other words, this method is used to attenuate only the direct coupling component, and the attenuation of the multipath components is done in the digital domain. The proposed method for RF cancellation is observed to perform better than the more traditional approach used in, e.g., [20] and [31]. The main benefit of this kind of RF cancellation process is most likely the increased accuracy of the cancellation signal in comparison to having only one line with a tunable delay, assuming a sufficiently accurate adaptation process to calculate the necessary parameters.

2.4.3 Analog-to-digital conversion

Another bottleneck, in addition to the RF components, are the analog-to-digital converters (ADCs). They are designed so that they utilize the whole dynamic range available when quantizing the signal. In the presence of strong SI, the ADC must use a certain amount of bits to describe a much larger range of voltage values, as opposed to a case where there is no SI. Thus, because the SI signal has a significantly larger amplitude than the signal of interest, the weaker signal has a very small effective resolution after the analog-to-digital conversion [59]. It is hence important to mitigate SI already before sampling the signal, in order to be able to implement a fully functional full-duplex transceiver.

For this reason, even if the analog-to-digital conversion is modeled as uniform quantization process without any non-idealities, it has a significant effect in terms of enabling full-duplex communication. Namely, the level of the quantization noise floor is constant for a fixed number of bits, and thus it is important to be able to provide sufficient gain for the signal before the ADC. Otherwise, the signal of interest might have insufficient SINR after digital cancellation, thus deteriorating the performance below the required level. However, if the power of the SI is too high, it might not be possible to amplify the signal by a sufficient amount. Namely, if the voltage range of the signal entering the ADC goes above a specified limit, the signal will be clipped. This distorts the signal heavily, and it might be impossible to recover it afterwards. Thus, it is important to attenuate the SI also before the ADC, for the signal of interest to have sufficient bit resolution after digital cancellation.

2.4.4 Digital cancellation

Similar to RF cancellation, the amount of achievable digital cancellation is also dependent on the quality of the SI channel estimate. However, since the reference samples for digital cancellation exist only in the digital domain, they do not include any nonlinear distortion occurring in the transceiver chain. Thus, if only linear signal processing methods are used, the nonlinearly distorted part of the SI signal cannot be attenuated. Effectively, this decreases the amount of achievable digital cancellation. However, by utilizing nonlinear processing techniques, it is possible to also cancel a nonlinearly distorted SI signal in the digital domain. This type of nonlinear digital cancellation algorithms have been recently reported, e.g., in [8,12,15,41]. In addition, for there to be anything left after digital SI cancellation, the resolution of the ADC must be sufficiently high, as otherwise the signal of interest will be lost below the quantization noise floor.

The performance of digital cancellation is also dependent on the chosen method for channel estimation, as well as on the length of the channel estimate. If the required amount of digital cancellation is high, the quality of the channel estimate must also be very good. This, on the other hand, means that the estimation procedure must have a sufficient amount of training data available to produce an accurate result. In addition, the length of the channel estimate filter must also be sufficiently long. Thus, if the required amount of digital cancellation is high, the computational complexity of the channel estimation procedure is increased, alongside with the system overhead in the form of increased amount of training data.

In this thesis, however, the emphasis is not on this kind of implementation issues, and they will not be analyzed in detail. Instead, the achieved amount of linear digital cancellation is chosen arbitrarily, and the actual requirements for the chosen performance level are not considered. This is a justifiable decision, as there are several studies available where the realized performance of linear digital SI cancellation is reported [20, 26, 27, 31]. Thus, the results of these studies are utilized when choosing a feasible value for the amount of digital cancellation.

2.4.5 Overall effect of non-idealities

As a result of these non-idealities and imperfections in the SI cancellation process, there will be residual self-interference left at detection stage. As can be observed from (2.2), this will decrease the capacity of the full-duplex communications channel. It is thus inevitable that the spectral efficiency achievable with a full-duplex transceiver, in comparison to traditional half-duplex systems, is never doubled. However, with more efficient SI cancellation mechanisms, the capacity can nevertheless be increased significantly. Furthermore, in order to enable the full-duplex operation

in the first place, a certain amount of SI must be cancelled in the analog domain. This way the power of nonlinear distortion and quantization noise will be on a reasonable level with respect to the signal of interest, and decoding the data is possible.

In literature, very promising practical full-duplex radio implementations have been reported [20, 27, 31, 62]. In these papers, radio frequency (RF) techniques are proposed for SI mitigation, in addition to digital signal processing techniques. Nearly 70 to 80 dB of attenuation has been reported at best, but in real-world scenarios the amount of achieved SI-mitigation is obviously somewhat less [31]. To make things more complex, practical small transceivers have RF components that do not work as ideally as the components used, e.g., in the setups of [20, 27, 31, 62]. For example, the amplifiers in the receiver will cause nonlinear distortion to the SI signal, which can significantly degrade the performance of a full-duplex transceiver if the level of the SI signal is too high.

3. FULL-DUPLEX TRANSCEIVER MODEL

The chosen approach is to model a complete full-duplex transceiver component by component, which allows the analysis regarding the feasibility of single-channel full-duplex communication in modern radios. Most of the emphasis in the calculations is at the receiver side since it is the more delicate part of the transceiver in terms of enabling full-duplex operation. It largely determines how well the transceiver can operate under powerful self-interference coming from the transmitter side. Nevertheless, the effect of the transmitter is still discussed to some extent since it also produces distortion which must be considered. A block diagram representing the analyzed full-duplex transceiver can be seen in Fig. 3.1. In particular, the analyzed transceiver is assumed to follow a direct-conversion architecture. This decreases the complexity of the electronics and also makes the analysis easier.

Another significant aspect of the full-duplex transceiver is the reference signal path for RF cancellation. In this thesis, two different scenarios are analyzed: one in which the reference signal is taken from the output of the PA and attenuated to a proper level, and one in which the reference signal is taken directly from the input of the PA. The scenarios are referred to as *Case A* and *Case B*, respectively. These two different reference signal paths are also marked in the block diagram. In Fig. 3.1 a switch is used to depict the selection between Case A and Case B.

The parameters of the individual components are chosen to correspond to a modern wireless transceiver, especially in terms of the considered wide bandwidth. Furthermore, the values for analog and digital SI cancellation are chosen to be the highest presented values reported in recent literature [31]. This means that the achieved total SI cancellation is somewhat optimistic. However, the presented calculations can easily be extended also to lower values of self-interference cancellation.

3.1 Receiver

RF cancellation

After the signal, received by the antenna, enters the actual receiver chain, the first operation to be performed is analog SI cancellation, or RF cancellation. The path loss between the transmit and receive antennas already significantly attenuates the SI signal, but also RF cancellation is required to prevent the saturation of the RF front-end. It is assumed that RF cancellation mitigates only the main component of the transmitted signal, according to [20] and [31]. The cancellation is done by tuning the delay and attenuation of the reference transmit signal, to match the

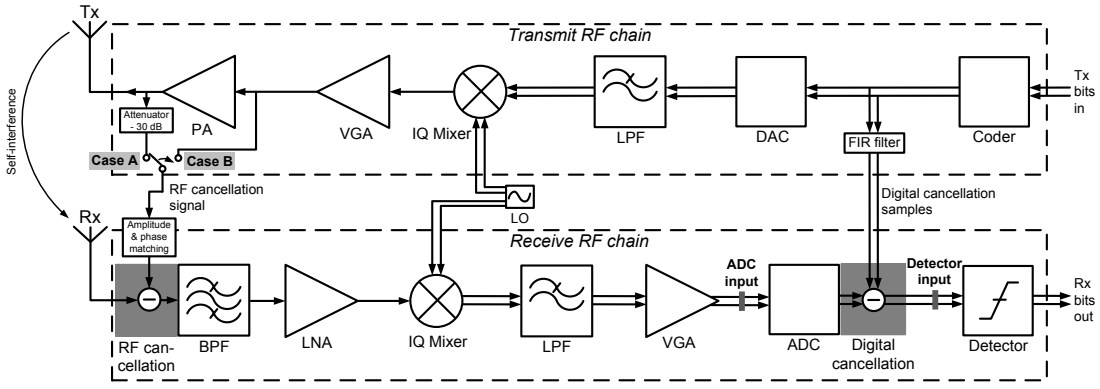

Figure 3.1: Block diagram of the analyzed direct-conversion full-duplex transceiver.

coupling path between the antennas, and then subtracting this reference signal from the received signal. Furthermore, in the analysis, two alternatives for the reference signal path are considered, referred to as Case A and Case B.

- Case A describes perhaps the most widely used implementation technique for taking the reference signal for RF cancellation [17, 20, 31, 42, 50]. Here, the reference signal is taken from the output of the PA, and thus also the possible distortion produced by the PA is included in the cancellation signal. This means that the PA-induced nonlinearities are attenuated by RF cancellation. However, the drawback of this approach is the need for an RF attenuator to achieve sufficiently low power level for the cancellation signal. The required amount of attenuation is obviously the estimated path loss between the antennas, as this ensures that the powers of the reference signal and SI signal are of similar magnitude at the RF cancellation block.

- In Case B, the reference signal is taken from the input of the PA, where the signal has not yet been amplified by the PA. As the gain of the PA is usually of similar magnitude as the path loss between the antennas, the required amount of attenuation for the reference signal is relatively small, and it can be achieved with a tunable amplitude & phase matching circuit [2]. Thus, no additional RF attenuator is required, resulting in a simpler and cheaper RF front-end. The problem in this technique is the nonlinear distortion produced by the PA, which is not included in the reference signal. Thus, it will not be attenuated by RF cancellation like in Case A, resulting in lower SINR in the analog domain. In addition, Case B is somewhat similar to the method used in [26] and [62], where a separate TX chain was used to generate the reference signal. Assuming that only the PA creates significant amounts of distortion to the signal, Case B can be used to model also this method, and the results obtained with Case B can be generalized also to this type of scenarios.

BPF and LNA

After the RF cancellation stage, the analyzed receiver follows a typical direct-conversion architecture. First, the signal is filtered with a passive band pass filter (BPF). As the filter is passive, it is assumed that its gain in the passband is 0 dB and that it is highly linear. For this reason, the possible distortion caused by the bandpass filter is assumed to be negligible.

After the band filtering, a low noise amplifier (LNA) is used to amplify the signal. The first LNA creates only 3rd-order nonlinear distortion to the in-band signal as it is still at the radio frequency. In general, the LNA creates odd-order nonlinear distortion, but in this experiment it is sufficient to assume that higher than 3rd-order distortion is negligibly weak.

IQ mixer and LPF

After the first amplification stage, the signal is downconverted to the baseband by an IQ mixer. The mixer is assumed to be active, and thus it also amplifies the signal. A local oscillator signal at the center frequency of the information signal is fed to the mixer. It is assumed that there is no significant leakage from the oscillator to the information signal path, and that the effects of phase noise and IQ imbalance are negligible. The mixer produces 2nd-order nonlinear distortion to the baseband, which overlaps with the signal of interest after downconversion. In addition, the mixer also produces 3rd-order nonlinear distortion which falls on to the signal band.

When the signal has been downconverted to the baseband, it is filtered with a low pass filter (LPF) in order to filter out all the spurs that are not in the signal band. Also this filter is assumed to be a completely linear passive filter with a gain of 0 dB. The mitigation of the adjacent channels is in practice done by this filter.

VGA and ADC

The final component before the ADC is the variable gain amplifier (VGA). In reality, it might consist of several amplifiers but in this analysis it is sufficient to model it as a single component. The gain of the VGA is tunable and its task is to amplify the signal to a predetermined power level. In addition, it is assumed that both the 2nd and 3rd-order distortion produced by the VGA will fall on the signal band.

An automatic gain control (AGC) algorithm tunes the gain of the VGA such that the full available voltage range of the ADC is utilized by the amplified signal and that its average power at the input of the ADC is constant. However, as signals with high peak-to-average-power ratio (PAPR) are considered in the analysis, a certain backoff is included in the amplification requirements so that the probability of clipping at the ADC is minimized. In this experiment, the ADC is assumed to be ideal, producing only quantization noise.

Digital cancellation

After the ADC, the remaining SI is mitigated in the digital domain by subtracting the transmitted baseband waveform from the received signal. The subtracted samples are generated by filtering the transmitted symbols with the linear estimate of the SI channel response. The channel estimation at this stage includes the effects of the transmitter, the coupling channel between the antennas, and the receiver. Also the multipath components are taken into account, unlike in RF cancellation. However, as only linear processing is used, the nonlinearly distorted component of the SI signal cannot be attenuated.

3.2 Transmitter

Similar to the receiver side, also the transmitter is chosen to have a direct-conversion architecture. Hence the structure of the transmitter is simpler and allows an easier analysis. A block diagram of the transmitter can be seen on the upper part of Fig 3.1.

When analyzing the transmitter chain, it is assumed that the power of thermal noise is negligibly low. This is a reasonable assumption as transmitters are usually not limited by the thermal noise floor. Hence, thermal noise is omitted in the analysis of the transmitter, and the noise figures of the components do not affect the calculations. Furthermore, only 3rd-order nonlinear distortion is considered when analyzing the transmitter.

DAC, IQ mixer, and VGA

The reference samples for digital cancellation are taken from the input of the digital-to-analog converter (DAC). After this, the digital samples are converted into analog domain by the DAC. The analog baseband signal is first filtered with a low pass filter (LPF) to attenuate the possible out-of-band distortion produced by the DAC. Again, it is assumed that the filter is passive and thus completely linear. After this, the signal is upconverted to radio frequency by an active IQ mixer, meaning that the mixer also amplifies the signal.

The upconverted signal is then amplified with a variable gain amplifier (VGA). The gain of the VGA is set so that the power of the signal at its output is the desired transmit power, excluding the gain of the PA. Thus, the desired transmit power is achieved by tuning the amplification of the VGA accordingly.

PA

The final component of the transmitter chain is the power amplifier (PA). It has fixed gain and it amplifies the signal to the actual transmit power level, and it is typically heavily nonlinear [29, 49, 51]. In our analysis, it is assumed that the PA produces 3rd-order distortion which falls on to the signal band, since this is the dominant distortion in practice. This is characterized with the IIP3 figure of the PA.

In theory, it is possible to decrease the power of the nonlinear distortion by decreasing the gain of the PA. However, this would also decrease the energy efficiency of the PA, which is obviously highly undesired [33]. Thus, there is a fundamental tradeoff between the linearity and energy efficiency of an amplifier. However, investigating this tradeoff in detail in terms of full-duplex communications is out of the scope of this thesis, and, for this reason, a typical PA is considered.

In Case A, where the reference signal for RF cancellation is taken from the output of the PA, nonlinear distortion is included in the reference signal, and can thus be compensated by RF cancellation. In Case B, however, the reference signal is taken from the input of the PA, and thus the nonlinearities produced by the PA remain on the same level after RF cancellation, as they are only attenuated by the coupling channel path loss. The possible nonlinearities of transmit chain mixer and VGA can be essentially omitted since these are part of the RF cancellation reference signal in both cases, and hence efficiently suppressed below the noise floor. Thus, it is sufficient to consider only the nonlinearities of the PA when analyzing the transmitter.

Another observation about the nonlinearities of the transmitted signal is that linear digital cancellation cannot suppress them. The reason for this is that the reference symbols for digital cancellation exist only in the digital domain and do not include any analog distortion. Moreover, nonlinear distortion cannot be modelled with a linear filter, and thus linear digital cancellation is unable to mitigate it.

3.3 Signal model

Based on the previous discussion about the structure of the transceiver chain, it is possible to write a detailed signal model for the total received signal. Let us denote the undistorted transmit signal by $x(t)$. As already discussed, the possible distortion caused by the IQ mixer and VGA of the transmit chain are omitted from the analysis. Thus, the signal at the input of the PA can be written as $\sqrt{g_{\text{tx}}}x(t)$, where g_{tx} is the combined gain of the IQ mixer and VGA.

The PA distorts the signal nonlinearily, and the signal at its output can be written as follows:

$$x_{\mathrm{PA}}(t) = \sqrt{g_{\mathrm{PA}}}\sqrt{g_{\mathrm{tx}}}x(t) + x_{\mathrm{NL,PA}}(t), \tag{3.1}$$

where g_{PA} is the power gain of the PA, and $x_{\mathrm{NL,PA}}(t)$ represents the nonlinear distortion produced by the PA. Denoting the coupling channel between the transmit and receive antennas as $h(t)$, the total received signal can be written as follows:

$$y_{\mathrm{tot}}(t) = y_{\mathrm{SOI}}(t) + h(t) \star \sqrt{g_{\mathrm{PA}}}\sqrt{g_{\mathrm{tx}}}x(t) + h(t) \star x_{\mathrm{NL,PA}}(t) + n(t), \tag{3.2}$$

where $y_{\mathrm{SOI}}(t)$ is the received signal of interest, and $n(t)$ is thermal noise. Next, RF cancellation is performed on this signal, and as a result we get

$$\begin{aligned} y_{\mathrm{tot,RF}}(t) = {} & y_{\mathrm{SOI}}(t) + h(t) \star \sqrt{g_{\mathrm{PA}}}\sqrt{g_{\mathrm{tx}}}x(t) + h(t) \star x_{\mathrm{NL,PA}}(t) + n(t) \\ & - a_{RFC}(t) \star \sqrt{g_{\mathrm{PA}}}\sqrt{g_{\mathrm{tx}}}x(t) - k_{\mathrm{NL}}a_{RFC}(t) \star x_{\mathrm{NL,PA}}(t), \end{aligned} \tag{3.3}$$

where $a_{RFC}(t)$ is the single-tap estimate of the SI coupling channel used in RF cancellation, and k_{NL} is set to equal 1 for Case A or 0 for Case B. The purpose of k_{NL} is to define whether the nonlinear distortion produced by the PA is attenuated by RF cancellation (Case A) or not (Case B).

After this, the signal propagates through the receiver chain, where it is amplified, and also distorted nonlinearily. Modeling the nonlinear distortion again in an additive form, the signal at the input of the ADC can be expressed as

$$\begin{aligned} y_{\mathrm{ADC}}(t) = {} & \sqrt{g_{\mathrm{rx}}}(y_{\mathrm{SOI}}(t) + (h(t) - a_{RFC}(t)) \star \sqrt{g_{\mathrm{PA}}}\sqrt{g_{\mathrm{tx}}}x(t) \\ & + (h(t) - k_{\mathrm{NL}}a_{RFC}(t)) \star x_{\mathrm{NL,PA}}(t) + n(t)) + x_{\mathrm{NL,2nd}}(t) \\ & + x_{\mathrm{NL,3rd}}(t) + n_{\mathrm{NF}}(t) \\ = {} & \sqrt{g_{\mathrm{rx}}}(y_{\mathrm{SOI}}(t) + (h(t) - a_{RFC}(t)) \star \sqrt{g_{\mathrm{PA}}}\sqrt{g_{\mathrm{tx}}}x(t) \\ & + (h(t) - k_{\mathrm{NL}}a_{RFC}(t)) \star x_{\mathrm{NL,PA}}(t)) + x_{\mathrm{NL,2nd}}(t) \\ & + x_{\mathrm{NL,3rd}}(t) + \sqrt{g_{\mathrm{rx}}}n(t) + n_{\mathrm{NF}}(t) \\ = {} & \sqrt{g_{\mathrm{rx}}}(y_{\mathrm{SOI}}(t) + (h(t) - a_{RFC}(t)) \star \sqrt{g_{\mathrm{PA}}}\sqrt{g_{\mathrm{tx}}}x(t) \\ & + (h(t) - k_{\mathrm{NL}}a_{RFC}(t)) \star x_{\mathrm{NL,PA}}(t)) + x_{\mathrm{NL,2nd}}(t) \\ & + x_{\mathrm{NL,3rd}}(t) + n_{\mathrm{tot}}(t), \end{aligned} \tag{3.4}$$

where g_{rx} is the total power gain of the receiver chain, $x_{\mathrm{NL,2nd}}(t)$ is the 2nd-order nonlinear distortion produced by the receiver chain, $x_{\mathrm{NL,3rd}}(t)$ is the 3rd-order nonlinear distortion, and $n_{tot}(t) = \sqrt{g_{\mathrm{rx}}}n(t) + n_{\mathrm{NF}}(t)$ is the total noise, $n_{\mathrm{NF}}(t)$ being the additional noise produced by the receiver chain according to its noise figure F.

The final procedure before the detection of the signal is digital SI cancellation. By denoting the channel estimate of the total SI channel with $\sqrt{g_{\mathrm{rx}}}\sqrt{g_{\mathrm{PA}}}\sqrt{g_{\mathrm{tx}}}a_{\mathrm{DC}}(n)$, the signal at the input of the detector can be written as

$$\begin{aligned} y_{\mathrm{D}}(nT_{\mathrm{s}}) &= \sqrt{g_{\mathrm{rx}}}(y_{\mathrm{SOI}}(nT_{\mathrm{s}}) + (h(nT_{\mathrm{s}}) - a(nT_{\mathrm{s}})) \star \sqrt{g_{\mathrm{PA}}}\sqrt{g_{\mathrm{tx}}}x(nT_{\mathrm{s}}) \\ &\quad + (h(nT_{\mathrm{s}}) - k_{\mathrm{NL}}a(nT_{\mathrm{s}})) \star x_{\mathrm{NL,PA}}(nT_{\mathrm{s}})) + x_{\mathrm{NL,2nd}}(nT_{\mathrm{s}}) \\ &\quad + x_{\mathrm{NL,3rd}}(nT_{\mathrm{s}}) + n_{\mathrm{tot}}(nT_{\mathrm{s}}) + n_{\mathrm{q}}(nT_{\mathrm{s}}) - \sqrt{g_{\mathrm{rx}}}\sqrt{g_{\mathrm{PA}}}\sqrt{g_{\mathrm{tx}}}a_{\mathrm{DC}}(n) \star x(nT_{\mathrm{s}}) \\ &= \sqrt{g_{\mathrm{rx}}}(y_{\mathrm{SOI}}(nT_{\mathrm{s}}) + (h(nT_{\mathrm{s}}) - a(nT_{\mathrm{s}}) - a_{\mathrm{DC}}(n)) \star \sqrt{g_{\mathrm{PA}}}\sqrt{g_{\mathrm{tx}}}x(nT_{\mathrm{s}}) \\ &\quad + (h(nT_{\mathrm{s}}) - k_{\mathrm{NL}}a(nT_{\mathrm{s}})) \star x_{\mathrm{NL,PA}}(nT_{\mathrm{s}})) + x_{\mathrm{NL,2nd}}(nT_{\mathrm{s}}) \\ &\quad + x_{\mathrm{NL,3rd}}(nT_{\mathrm{s}}) + n_{\mathrm{tot}}(nT_{\mathrm{s}}) + n_{\mathrm{q}}(nT_{\mathrm{s}}), \end{aligned} \tag{3.5}$$

where T_{s} is the sampling interval, and $n_{\mathrm{q}}(t)$ is the quantization noise. The terms $(h(nT_{\mathrm{s}}) - a(nT_{\mathrm{s}}) - a_{\mathrm{DC}}(n))$ and $(h(nT_{\mathrm{s}}) - k_{\mathrm{NL}}a(nT_{\mathrm{s}}))$ provide a certain amount of attenuation for the linear SI and PA-induced nonlinear distortion, and their level can be denoted in a simplified scenario by a scalar.

Equation (3.5) represents the final form of the total signal at the input of the detector, which includes all the SI cancellation stages. Thus, the achieved SINR is calculated based on (3.5), meaning that this equation reveals the overall peformance of the full-duplex transceiver.

4. SYSTEM CALCULATIONS

The analysis of the full-duplex transceiver is performed with system calculations. This allows the inspection of the individual signal components and their respective power levels. Thus, it can be observed which distortion component is the dominant one and should thereby be attenuated by some means. Also, the total SINR at the detector input is studied, as it reveals the overall performance of the transceiver.

It is assumed in all the calculations that if the effective noise power more than doubles because of SI, the throughput of the transceiver becomes too low. For this reason, the SINR under FD operation is compared to the SINR under HD operation, which is assumed to be approximately the same as signal-to-thermal-noise-ratio (SNR_{d}) at the input of the detector. If the difference is greater than 3 dB, the noise power has more than doubled due to SI, and it is assumed that the throughput requirement cannot be fulfilled. In other words, the maximum allowed SINR loss is 3 dB. The transmit power, with which this point is reached, is referred to as the *maximum transmit power*. It is marked to the relevant figures with a vertical line to illustrate what is effectively the highest transmit power with which the full-duplex transceiver can still operate with sufficient performance.

4.1 Signal components

In the transceiver system calculations, the two most relevant interfaces are the *ADC input* and *detector input*. These points are also marked in the block diagram in Fig. 3.1. Furthermore, example signal characteristics and the different signal components, alongside with their typical relative power levels, are illustrated in Fig. 4.1. The reason for the significance of the ADC input is the role of quantization and its dependence on self-interference. As the receiver automatic gain control (AGC) keeps the total ADC input at constant level, higher noise plus self-interference power means reduced desired signal power and thus more and more of the ADC dynamic range is reserved by the SI signal. This, in turn, indicates reduced effective resolution for the desired signal which may limit the receiver performance.

The effect of quantization is studied by determining the SINR at the ADC input, quantifying the power of the desired signal relative to the other signal and distortion components at this point. A typical situation in terms of the power levels at this interface can be seen on the left in Fig. 4.1, where the SI signal is clearly dominating, and thus reserving a signicant amount of dynamic range.

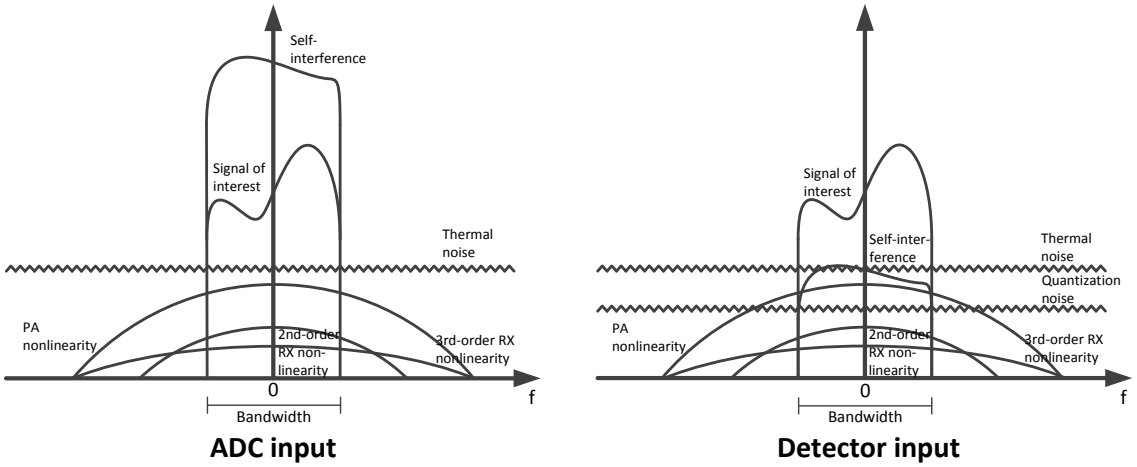

Figure 4.1: An illustration of the signal spectra at the input of the ADC and the detector.

Then, to characterize the overall performance of the whole full-duplex transceiver, and how different types of distortion affect it, also the final SINR at the detector input, including the effect of digital SI cancellation, is studied and analyzed. This is thus the other significant point or calculation interface in the forthcoming analysis. Typical power levels also at this interface can be seen on the right in Fig. 4.1, where the SI signal has now been attenuated by digital cancellation, and it is not such a significant distortion component at this point. However, due to analog-to-digital conversion, there is now quantization noise in the total signal, which might be a significant issue, depending on the parameters of the transceiver.

Throughout the rest of this thesis, it is assumed that all the distortion types can be modelled in additive form. This is very typical in transceiver system calculations, e.g., see [29,51]. The good accuracy of this approach is also verified by full waveform simulations presented in Section 6.

Based on (3.4), and taking into account the above assumptions, an equation for the SINR at the input of the ADC can be determined. By dividing the power of the signal of interest with the total power of the noise and interference components at the input of the ADC, we arrive at the following expression for the SINR in linear scale:

$$sinr_{\mathrm{ADC}} = \frac{g_{\mathrm{rx}} p_{\mathrm{SOI,in}}}{g_{\mathrm{rx}} F p_{\mathrm{N,in}} + \frac{g_{\mathrm{rx}}}{a_{\mathrm{ant}}} \left(\frac{p_{\mathrm{tx}}}{a_{\mathrm{RF}}} + \frac{p_{\mathrm{3rd,PA,tx}}}{a_{\mathrm{NL}}} \right) + p_{\mathrm{2nd}} + p_{\mathrm{3rd}}}, \tag{4.1}$$

where

- $p_{\mathrm{SOI,in}}$ is the power of the signal of interest at the input of the receiver ($y_{\mathrm{SOI}}(t)$)
- $p_{\mathrm{N,in}}$ is the thermal noise power at the input of the receiver ($n(t)$)
- a_{ant} and a_{RF} are the amounts of antenna attenuation and RF cancellation

- p_{tx} is the transmit power
- $p_{\mathrm{3rd,PA,tx}}$ is the power of PA-induced nonlinear distortion at the output of the transmit chain ($x_{\mathrm{NL,PA}}(t)$)
- a_{NL} is a_{RF} for Case A and 1 for Case B ($k_{\mathrm{NL}} = 1$ and $k_{\mathrm{NL}} = 0$, respectively)
- p_{2nd} and p_{3rd} are the cumulative powers of 2nd- and 3rd-order nonlinear distortion produced at the receiver chain ($x_{\mathrm{NL,2nd}}(t)$ and $x_{\mathrm{NL,3rd}}(t)$).

All the powers are assumed to be in linear units in this equation, which is indicated also by the lowercase letters. These signal components are illustrated on the left in Fig. 4.1 with realistic relative power levels.

The purpose of defining the input SINR of the ADC is to quantify the ratio of the useful signal power and total noise plus interference power entering the analog-to-digital interface. With fixed ADC voltage range, and assuming that the overall receiver gain is controlled properly, the total ADC input power

$$p_{ADC,in} = g_{\mathrm{rx}} p_{\mathrm{SOI,in}} + g_{\mathrm{rx}} F p_{\mathrm{N,in}} + \frac{g_{\mathrm{rx}}}{a_{\mathrm{ant}} a_{\mathrm{RF}}} p_{\mathrm{tx}} + \frac{g_{\mathrm{rx}}}{a_{\mathrm{NL}}} p_{\mathrm{3rd,PA,tx}} + p_{\mathrm{2nd}} + p_{\mathrm{3rd}}$$

is always matched to the maximum allowed average power, say p_{target}. This will be elaborated in more detail later.

Next, based on (3.5), the SINR at the detector input can be defined as

$$sinr_{\mathrm{D}} = \frac{g_{\mathrm{rx}} p_{\mathrm{SOI,in}}}{g_{\mathrm{rx}} F p_{\mathrm{N,in}} + \frac{g_{\mathrm{rx}}}{a_{\mathrm{ant}}} \left(\frac{p_{\mathrm{tx}}}{a_{\mathrm{RF}} a_{\mathrm{dig}}} + \frac{p_{\mathrm{3rd,PA,tx}}}{a_{\mathrm{NL}}} \right) + p_{\mathrm{quant}} + p_{\mathrm{2nd}} + p_{\mathrm{3rd}}}, \tag{4.2}$$

where a_{dig} is the attenuation achieved by digital cancellation ($h(nT_{\mathrm{s}}) - a(nT_{\mathrm{s}}) - a_{\mathrm{DC}}(nT_{\mathrm{s}})$) and p_{quant} is the power of quantization noise ($n_{\mathrm{q}}(nT_{\mathrm{s}})$). This SINR defines the overall receiver performance of the full-duplex transceiver and is thus the most significant figure of merit in the analysis. A realistic sketch of the relative power levels of the specified signal components also at this interface can be seen on the right in Fig. 4.1.

The following subsections analyze in detail the different component powers of the above two principal equations, and their dependence on the transmit power, RF cancellation, digital cancellation and TX and RX chain nonlinear characteristics. Then, in Section 5, these are all brought together and it is analyzed in detail how varying these elementary parameters and transceiver characteristics affects the SINR at both of the studied interfaces and thereon the whole transceiver operation.

4.2 Elementary equations

The basic operation of the transceiver can be modelled with certain elementary equations. These include the sensitivity level and noise figure of the receiver, the signal-to-noise ratio of the ADC, and the simplified equations used to calculate the power of nonlinear distortion.

4.2.1 RF front-end

The sensitivity of the receiver is determined by the thermal noise floor, the noise figure of the receiver, and the SNR requirement at the detector. These parameters are selected so that they produce the desired throughput. It is important to note that the degradation of SINR caused by SI is not taken into account when calculating sensitivity. This is based on the assumption that SI can be mitigated sufficiently so that it does not raise the noise floor significantly. It is also easier to compare the performance of the receiver with and without SI when the sensitivity can be assumed to be the same in each scenario.

In order to determine the sensitivity level of the receiver in decibels per milliwatt (dBm), the following equation can be used [29]:

$$P_{\text{sens}} = -174 + 10\log_{10}(B) + NF_{\text{rx}} + SNR_{\text{d}}, \tag{4.3}$$

where B is the bandwidth of the system in Hertz, NF_{rx} is the noise figure of the receiver, and SNR_{d} is the signal-to-noise-ratio requirement at the input of the detector.

In modern transceivers, the sensitivity is obviously affected by the chosen code rate and modulation, but the effect of these parameters is omitted in these calculations. This does not affect the reliability of the results, as calculating the sensitivity with (4.3) provides a good baseline figure. However, the meaning of the sensitivity is now interpreted as the minimum received signal power with which it is possible to achieve certain throughput.

The total noise factor of the receiver chain can be calculated using Friis' formula [29] as

$$F_{rx} = F_{\text{LNA}} + \frac{F_{\text{mixer}} - 1}{g_{\text{LNA}}} + \frac{F_{\text{VGA}} - 1}{g_{\text{LNA}} g_{\text{mixer}}}, \tag{4.4}$$

where F_{LNA}, F_{mixer}, and F_{VGA} are the noise factors of the LNA, IQ Mixer, and VGA, respectively. Similarly, g_{LNA}, g_{mixer}, and g_{VGA} are the respective linear gains of these components. The noise figure in decibels can be obtained directly from the noise

factor as

$$NF_{\text{rx}} = 10\log_{10}(F_{\text{rx}}). \tag{4.5}$$

In this analysis, the power of the actual received signal is chosen to be only slightly above the sensitivity level. This represents a challenging scenario for the receiver, because the power of the received signal of interest is low, while the power of SI is very high.

4.2.2 Quantization noise

It will be shown later that the quantization noise produced by the ADC is a significant concern in full-duplex transceivers. The SNR of the ADC can be calculated using the following well known equation [29]:

$$SNR_{\text{ADC}} = 6.02b + 4.76 - PAPR, \tag{4.6}$$

where b is the number of bits at the ADC, and $PAPR$ is the estimated peak-to-average power ratio. The above expression assumes proper AGC at ADC input such that the full range of the ADC is used but the clipping of the signal peaks is avoided. However, the analysis could be easily translated to cover clipping noise as well [59]. The absolute power level of the quantization noise can be determined based on (4.6), when the power of the total signal is known.

4.2.3 Nonlinear distortion at the receiver

In addition to quantization noise, the nonlinear distortion produced by the components of the transceiver is of great interest. In these calculations, the nonlinearities are modelled by using the $IIP2$ and $IIP3$ figures (2nd and 3rd-order input-referred intercept points). They are based on the knowledge that the power of nonlinear distortion increases faster with respect to input power than the power of the actual fundamental signal.

The logarithmic power curves of nonlinear distortion and the fundamental signal can be seen from Fig. 4.2. The slope of the power curve is two for the 2nd-order distortion and three for the 3rd-order distortion, assuming that the slope of the fundamental curve is one. The point, at which the nonlinear distortion is equally strong with the fundamental signal component, is referred to as the intercept point. It must be noted, however, that this point cannot be reached in reality. It can only be determined by means of extrapolation based on the respective power levels at lower input powers. When the intercept point is expressed in terms of input power, it is referred to as nth order input intercept point ($IIPn$), n being the order of the nonlinear component in question.

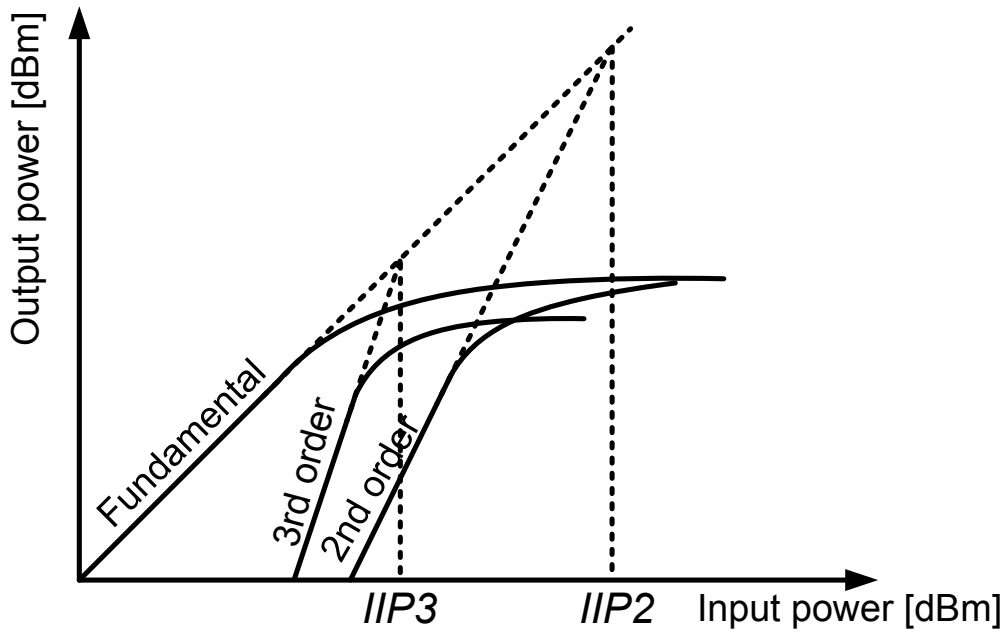

Figure 4.2: The relative power levels of 2nd and 3rd-order nonlinear distortion. The horizontal axis depicts the input power while the vertical axis depicts the output power. The power levels are expressed in dBm.

For nth-order nonlinearities, the power of the distortion in decibels per milliwatt (dBm) is obtained from

$$P_{\text{nth}} = P_{\text{out}} - (n-1)(IIPn - P_{\text{in}}) \tag{4.7}$$

where P_{in} is the total input power of the component and P_{out} is the total output power, both in dBm. This equation can be directly obtained from Fig. 4.2 for 2nd and 3rd-order nonlinearities, based on the slopes of the power curves.

It is clear that calculating the power of nonlinear distortion in this manner is not ideally precise as this is a very simplified model. For example, the bandwidth of the distortion is not taken into account. This creates some error because in reality the filters attenuate those frequency components of the distortion that fall outside the passband. Furthermore, the slopes of the fundamental signal and the nonlinear distortion are not perfectly linear over the whole range of input powers. Also this creates some additional error in the model, especially with signals of higher power. However, as a first approach, this model is sufficient to estimate the effects of the nonlinearities in a full-duplex transceiver, and it also allows for the analysis to be conducted in terms of closed form expressions. Again, relatively good accuracy, e.g., over a wide range of transmit powers, is illustrated and verified through reference waveform simulations in Section 6.

4.3 Accumulated component powers at detector input

In order to analyze the receiver chain properly, the total accumulated power levels of the individual signal components at the input of the detector should be known. For this reason, equations are derived for each of them. First, the absolute power of quantization noise at the detector, based on (4.6), can be written as

$$\begin{aligned} P_{\text{quant}} &= P_{\text{target}} - SNR_{\text{ADC}} \\ &= P_{\text{target}} - 6.02b - 4.76 + PAPR, \end{aligned} \tag{4.8}$$

where P_{target} is the target average power of the signal at the ADC input such that clipping is avoided. Assuming that the PAPR of the signal is estimated to be constant, it can be observed that the power of the quantization noise depends only on the characteristics of the ADC, namely its maximum input power and the amount of bits.

The powers of the other signal components depend on several parameters, first and foremost on the total gain of the receiver chain. As the signal of interest, the SI signal, and the nonlinear distortion produced by the PA are the only significant signal components at the input of the receiver, the total gain in linear units can be written as

$$g_{\text{rx}} = \frac{p_{\text{target}}}{\frac{1}{a_{\text{ant}}}\left(\frac{p_{\text{tx}}}{a_{\text{RF}}} + \frac{p_{\text{3rd,PA,tx}}}{a_{\text{NL}}}\right) + p_{\text{SOI,in}}}. \tag{4.9}$$

When considering Case A, the nonlinear distortion produced by the PA is attenuated by RF cancellation. Thus, with high transmit powers, the total signal power at the input of the receiver can be approximated by the power of SI, as it is several magnitudes higher than the power of any other signal component when operating close to sensitivity level. In this case, the equation for the gain simplifies to

$$g_{\text{rx}} = \frac{a_{\text{ant}} a_{\text{RF}} p_{\text{target}}}{p_{\text{tx}}}. \tag{4.10}$$

The variability of the gain is in practice achieved by tuning the gain of the VGA, but in (4.9) and (4.10) the gain is expressed as a single figure for simplicity.

Knowing the total gain of the receiver, it is now trivial to write the equations for the powers of the other signal components at the input of the detector. The powers of the signal of interest and thermal noise can be written as

$$P_{\text{SOI}} = P_{\text{SOI,in}} + G_{\text{rx}} \tag{4.11}$$

$$P_{\text{N}} = P_{\text{N,in}} + G_{\text{rx}} + NF_{\text{rx}}. \tag{4.12}$$

The power of linear SI can be written as

$$P_{\mathrm{SI}} = P_{\mathrm{tx}} - A_{\mathrm{ant}} - A_{\mathrm{RF}} - A_{\mathrm{dig}} + G_{\mathrm{rx}}. \tag{4.13}$$

Furthermore, for high transmit powers, when (4.10) can be used to approximate the total gain of the receiver chain, the power of the SI signal becomes $P_{\mathrm{SI}} = P_{\mathrm{target}} - A_{\mathrm{dig}}$.

The total powers of the 2nd and 3rd-order nonlinear distortion produced by the receiver chain (in Watts) can be derived based on (4.7). The derivation is shown in detail in Appendix A, and the resulting equations can be written as follows:

$$p_{\mathrm{2nd}} \approx g_{\mathrm{LNA}}^2 g_{\mathrm{mixer}} g_{\mathrm{VGA}} p_{\mathrm{in}}^2 \left(\frac{1}{iip2_{\mathrm{mixer}}} + \frac{g_{\mathrm{mixer}}}{iip2_{\mathrm{VGA}}} \right) \tag{4.14}$$

$$p_{\mathrm{3rd}} \approx g_{\mathrm{LNA}} g_{\mathrm{mixer}} g_{\mathrm{VGA}} p_{\mathrm{in}}^3 \left[\left(\frac{1}{iip3_{\mathrm{LNA}}} \right)^2 + \left(\frac{g_{\mathrm{LNA}}}{iip3_{\mathrm{mixer}}} \right)^2 + \left(\frac{g_{\mathrm{LNA}} g_{\mathrm{mixer}}}{iip3_{\mathrm{VGA}}} \right)^2 \right], \tag{4.15}$$

where the subscript of each parameter indicates the considered component. Furthermore, $iip2_{\mathrm{k}}$ and $iip3_{\mathrm{k}}$ are the 2nd and 3rd-order input intercept points expressed in Watts, g_{k} is the linear gain of the corresponding component, and P_{in} is the total power of the signal after RF cancellation, again in Watts.

Certain approximations are made when deriving (4.14) and (4.15). Firstly, the increase in the noise floor occurring within each component is omitted from this analysis, as its effect is insignificant. In addition, some terms which were observed to be insignificantly small with realistic parameters were removed from the equations. The error caused by these approximations can be shown to be negligibly small with the chosen set of parameters. A detailed derivation of (4.14) and (4.15), as well as the error analysis, is given in Appendix A.

The power of the PA-induced nonlinear distortion at the output of the transmit chain can be written as

$$\begin{aligned} P_{\mathrm{3rd,PA,tx}} &= P_{\mathrm{tx}} - 2(IIP3_{\mathrm{PA}} - (P_{\mathrm{tx}} - G_{\mathrm{PA}})) \\ &= 3P_{\mathrm{tx}} - 2(IIP3_{\mathrm{PA}} + G_{\mathrm{PA}}), \end{aligned} \tag{4.16}$$

where $IIP3_{\mathrm{PA}}$ is the IIP3 figure of the PA and G_{PA} is the gain of the PA. This value is used, for example, in (4.9), as the gain is determined based on the signal levels at the input of the receiver chain. Using this, the power of the PA-induced nonlinear distortion at the input of the detector can then be written as

$$\begin{aligned} P_{\mathrm{3rd,PA}} &= P_{\mathrm{3rd,PA,tx}} + G_{\mathrm{rx}} - A_{\mathrm{ant}} - A_{\mathrm{NL}} \\ &= 3P_{\mathrm{tx}} - 2(IIP3_{\mathrm{PA}} + G_{\mathrm{PA}}) + G_{\mathrm{rx}} - A_{\mathrm{ant}} - A_{\mathrm{NL}}. \end{aligned} \tag{4.17}$$

In this analysis, it is assumed that nonlinear SI cancellation is not performed at the digital domain. Thus the nonlinear distortion produced by the PA is only attenuated by the coupling channel path loss (A_{ant}), and potentially by RF cancellation ($A_{\text{NL}} = A_{\text{RF}}$), if considering Case A.

After giving numerical values for the involved component and processing parameters, (4.8)–(4.17) can then be directly used to analyze and determine the receiver performance of a general full-duplex transceiver. The power levels of the signal components can be used, for example, to determine the SINR under various circumstances.

In order to study the requirements of the ADC in more detail, it is calculated how many bits are lost from the signal of interest because of SI. This is based on the notion that a powerful SI signal will reserve most of the dynamic range of the ADC and thus decrease the resolution of the desired signal. The amount of lost bits due to noise and interference can be determined by calculating how many decibels the signal of interest is below the total signal power, as this is directly the amount of dynamic range that is reserved by the noise and interference. The amount of lost bits can thus be calculated using the following equation:

$$b_{\text{lost,I+N}} = \frac{P_{\text{tot}} - P_{\text{SOI}}}{6.02}, \tag{4.18}$$

where P_{tot} and P_{SOI} are the total power of the signal and the power of the signal of interest at the input of the ADC, respectively, and 6.02 depicts the dynamic range of one bit, thus mapping the loss of dynamic range to loss of bits. In this analysis, the actual bit loss is defined as the increase in bit loss when assuming full-duplex operation, as opposed to a scenario where there would be no SI. Using (4.18), an equation for the defined bit loss can be derived. The derivation is shown in detail in Appendix B, and the final form of the equation can be written as

$$b_{\text{lost}} = \log_4 \left[1 + \left(\frac{1}{p_{\text{SOI,in}} + p_{\text{N,in}}} \right) \left(\frac{p_{\text{tx}}}{a_{\text{ant}} a_{\text{RF}}} + \frac{p_{\text{tx}}^3}{a_{\text{ant}} a_{\text{NL}} iip3_{\text{PA}}^2 g_{\text{PA}}^2} \right) \right]. \tag{4.19}$$

It is worth noting that when considering Case A, the role of the PA-induced nonlinear distortion is negligibly small at the ADC input and the 3rd-order term of p_{tx} can be omitted from (4.19). Nevertheless, for clarity, the equation for bit loss is presented here in its most general form. Hence, it is possible to calculate the bit loss directly with (4.19) using the chosen parameters.

4.4 Preliminary analysis

Some observations can already be made based on solely the derived system equations. The equations for the power levels of the signal of interest, thermal noise, and the SI signal, namely (4.11)–(4.13), are rather intuitive, as they are only affected by the gain and noise figure of the receiver, and the SI is attenuated by the different cancellation stages. However, the equations for the power levels of the 2nd and 3rd-order nonlinear distortion, namely (4.14)–(4.15), produced by the receiver chain, are more intriguing. It can be observed from the equations that the linearity of the VGA has the largest effect on the power of nonlinear distortion. This can be explained by the fact that the signal is at its strongest at the input of the VGA, which obviously indicates higher power also for nonlinear distortion.

The power of nonlinear distortion produced by the transmitter chain can be calculated in a very straightforward manner, as only the distortion produced by the PA has to be considered. Thus, (4.17) is in essence the direct definition for the power of nonlinear distortion. However, when observing the power of this signal component at the input of the detector, there is a major difference between Case A and Case B, as in the former it is attenuated by RF cancellation. Thus, in Case B the power of the nonlinear distortion produced by the PA is several magnitudes higher than in Case A.

When studying the equation for loss of bits due to SI, given in (4.19), the obvious observation is that increasing the transmit power with respect to the other signal components also increases the bit loss. Furthermore, increasing antenna attenuation or RF cancellation decreases the bit loss. These are relatively intuitive results, but with (4.19) they can be quantified and analyzed exactly. It is also important to note that the bit loss does not depend on the total amount of bits in the ADC. Thus the results obtained with (4.19) apply to all ADCs.

5. RESULTS AND ANALYSIS

The power levels of the different signal components can be calculated using (4.8)–(4.17). The calculations can be done with different parameters to see how each of them affects the relative power levels. First, the calculations are done under the assumption that the reference signal for RF cancellation is taken from the output of the PA (Case A). After that, it is assumed that the reference signal is taken from the input of the PA (Case B).

5.1 Parameters

The parameters that are used in this thesis are largely based on practical full-duplex implementations [20, 27, 31] and real transceiver implementations [14, 29, 47, 51, 70]. The intention is to model a realistic transceiver, having components suitable for mass production. For this reason, the requirements for the components cannot be too strict, as the cost of the device would then be too high.

5.1.1 Receiver

The general system level parameters of the studied full-duplex transceiver are shown in Table 5.1, and the parameters of the individual components of the receiver are shown in Table 5.2. Two sets of parameters are defined and they are referred to as Parameter Set 1 and Parameter Set 2. The first set of parameters depicts a reasonably state-of-the-art wideband transceiver. The parameters of the second set model a more challenging scenario with lower received signal power, decreased linearity, and slightly inferior SI cancellation ability. In most parts of the analysis, Parameter Set 1 is used as it depicts better the characteristics of modern transceivers, especially in terms of bandwidth and linearity.

With (4.3), the sensitivity level of the receiver can be calculated as $P_{\text{sens}} = -88.9$ dBm for Parameter Set 1, as shown in Table 5.1. This is a slightly pessimistic value compared to, for example, the reference sensitivity specified in the LTE specifications [1], where a sensitivity level of -97 dBm is given for QPSK modulation when using 10 MHz bandwidth. For Parameter Set 2, the sensitivity is calculated as $P_{\text{sens}} = -100.1$ dBm, which is similar to the values specified in LTE specifications when using 3 MHz bandwidth. However, the exact value of the sensitivity is of little importance, as long as it is within a realistic range. Also, the calculations can

Table 5.1: System level parameters of the full-duplex transceiver for Parameter Sets 1 and 2.

Parameter	**Value for Param. Set 1**	**Value for Param. Set 2**
SNR requirement	10 dB	5 dB
Bandwidth	12.5 MHz	3 MHz
Receiver noise figure	4.1 dB	4.1 dB
Sensitivity	-88.9 dBm	-100.1 dBm
Received signal power	-83.9 dBm	-95.1 dBm
Antenna separation	40 dB	40 dB
RF cancellation	40 dB	20 dB
Digital cancellation	35 dB	35 dB
ADC bits	8	12
ADC P-P voltage range	4.5 V	4.5 V
PAPR	10 dB	10 dB
Allowed SINR loss	3 dB	3 dB

Table 5.2: Parameters for the components of the receiver. The values in parentheses are the values used in Parameter Set 2.

Component	**Gain [dB]**	**IIP2 [dBm]**	**IIP3 [dBm]**	**NF [dB]**
BPF	0	-	-	0
LNA	25	43	-9 (-15)	4.1
Mixer	6	42	15	4
LPF	0	-	-	0
VGA	0-69	43	14 (10)	4
Total	31-100	11	-17 (-21)	4.1

Table 5.3: Parameters for the components of the transmitter.

Component	**Gain [dB]**	**IIP2 [dBm]**	**IIP3 [dBm]**	**NF [dB]**
LPF	0	-	-	0
Mixer	5	-	5	9
VGA	0-35	-	5	10
PA	27	-	20	5
Total	32-67	-	-20	10.3

be easily repeated with alternative parameters, if needed. Here, the power of the received signal is assumed to be 5 dB above sensitivity level, resulting in a received power level of either $P_{\mathrm{SOI,in}} = -83.9$ dBm or $P_{\mathrm{SOI,in}} = -95.1$ dBm, depending on the parameter set.

The isolation between the antennas is assumed to be 40 dB. This value, or a value of similar magnitude, has been reported several times in earlier literature [27,31,62]. The SI signal is further mitigated by RF cancellation. From Table 5.1 it can be observed that for Parameter Set 1 the amount of RF cancellation is 40 dB. This value is somewhat optimistic, as it was achieved in [31] under idealized conditions. In Parameter Set 2, a value of 20 dB is used for the amount RF cancellation which represents perhaps a more practical scenario.

The component parameters of the actual direct-conversion receiver chain are determined according to [14, 47, 70]. The objective is to select typical parameters for each component, and thus obtain reliable and feasible results. The chosen parameters are shown in Table 5.2, where the values without parentheses are used in Parameter Set 1 and the values with parentheses are selected when using Parameter Set 2. With (4.14) and (4.15), the total IIP2 and IIP3 figures of the whole receiver were calculated to be 10.8 dBm and -17.1 dBm (Parameter Set 1) or 10.8 dBm and -20.1 dBm (Parameter Set 2), respectively.

As already mentioned, the gain of the VGA is tuned so that the total average power of the signal has a constant value of 7 dBm at the input of the ADC. Furthermore, it is assumed that the PAPR of the signal is 10 dB. This corresponds to a peak amplitude of approximately 2.25 V when the input resistance of the ADC is 100 Ω. Hence, because no clipping is allowed, the total voltage range of the ADC is chosen to be 4.5 V as this corresponds to the peak-to-peak voltage of the signal and thus allows for the whole dynamic range to be utilized. According to [3], this is a feasible value for the ADC voltage range. Using (4.6), the signal to noise ratio of the analog-to-digital conversion can now be calculated as

$$SNR_{\mathrm{ADC}} = 6.02b + 4.76 - PAPR = 6.02b - 5.24,$$

where b is the number of bits at the ADC.

5.1.2 Transmitter

The parameters of the individual TX components are shown in Table 5.3, and they are the same for both parameter sets. Again, typical values are chosen for the parameters according to [29] and [51]. This ensures that the conclusions apply to a realistic TX chain. Furthermore, for the transmitter, only 3rd-order nonlinear distortion is taken into account as the 2nd-order nonlinearities do not fall on the

actual signal band. Assuming that the power of the feeding amplifier input signal is approximately −35 dBm, it can be observed from the table that, with the maximum feeding amplifier gain, the power of the 3rd-order nonlinear distortion at the output of the transmit chain is 40 dB lower than the fundamental signal component. Hence, the spectral purity of the considered TX chain is relatively high, and thus the obtained results, when it comes to the PA-induced nonlinear distortion, are on the optimistic side.

Taking into account the input power and maximum gain range of the feeding amplifier, it can also be observed From Table 5.3 that the power of the transmitted signal is between −8 and 27 dBm. This is a sufficient range for example in WLAN applications, or in other types of indoor communications. In addition, the studied transmit power range applies in some cases also to mobile devices in a cellular network, like class 3 LTE mobile transmitter [1]. In the following numerical results, the transmit power is varied between −5 and 25 dBm.

5.2 Results with Case A

In this section, calculations are performed and presented under the assumption that the reference signal for RF cancellation is taken from the output of the PA (Case A), and attenuated afterwards. Thus, the nonlinear distortion produced by the PA is included in the cancellation signal and it is also mitigated by RF cancellation.

5.2.1 Fixed amount of digital cancellation

In the first part of the analysis, Parameter Set 1 is used and only the transmit power of the transceiver is varied, while all the other parameters remain constant and unaltered. The power levels of the different signal components can be seen in Fig. 5.1 in terms of transmit power. The power levels have been calculated using (4.8)–(4.17) with the selected parameters.

It is imminently obvious that with the chosen parameters, the actual SI is the most significant distortion component. Furthermore, it can be observed that the maximum transmit power is approximately 15 dBm, marked by a vertical line. After this point, the loss of SINR due to SI becomes greater than 3 dB, because the SI becomes equally powerful with thermal noise. When interpreting the behavior of the curves in Fig. 5.1, one should also remember that the power of the signal entering the ADC is kept approximately constant by the AGC. Thus, in practise, the total gain of the RX chain reduces when transmit power increases.

The amount of lost bits, with respect to transmit power, can be seen in Fig. 5.2. The curve is calculated with (4.19) and it tells how much of the dynamic range of the ADC is effectively reserved by SI. It can be observed that when using Parameter

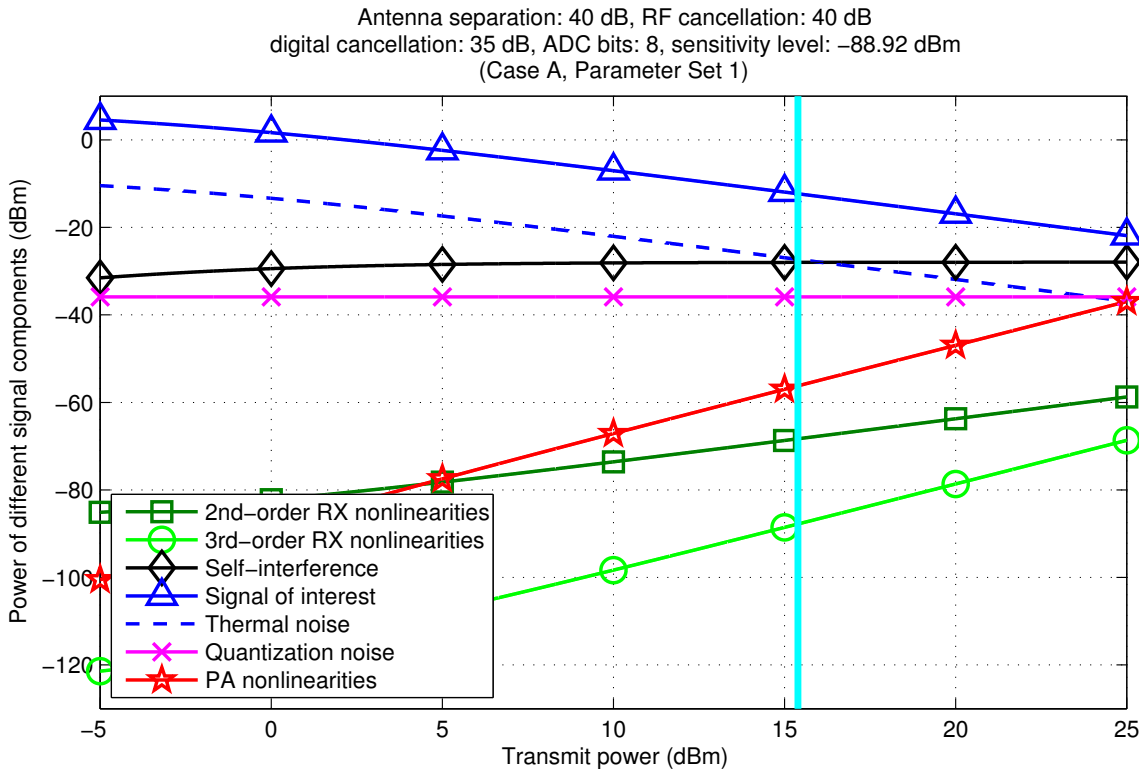

Figure 5.1: The power levels of different signal components at the input of the detector with Parameter Set 1.

Set 1, approximately 3 bits are lost due to SI with the maximum transmit power of 15 dBm. This emphasizes the fact that, in this scenario, the actual SI is the limiting factor for the transmit power. Actually, the power of quantization noise is almost 10 dB lower. However, from Fig. 5.2 it can also be observed that, with a transmit power of 20 dBm, the bit loss is already 4 bits. This indicates that, in order to enable the usage of higher transmit powers, high resolution is required for the ADCs.

5.2.2 Variable amount of digital cancellation

In order to further analyze the limits set by analog-to-digital conversion and non-linear distortion, in the second part of this analysis it is assumed that the amount of digital linear cancellation can be increased by an arbitrary amount, while the other parameters are chosen according to Parameter Set 1. With this assumption, it is possible to cancel the remaining SI perfectly in the digital domain. The reason for performing this type of an analysis is to determine the boundaries of digital signal processing (DSP) based SI cancellation, as it would be beneficial to cancel as large amount of SI in the digital domain as possible. However, in many cases, increasing only digital cancellation is not sufficient to guarantee high enough SINR, because nonlinear distortion and quantization noise will anyway increase the noise floor above the allowed level.

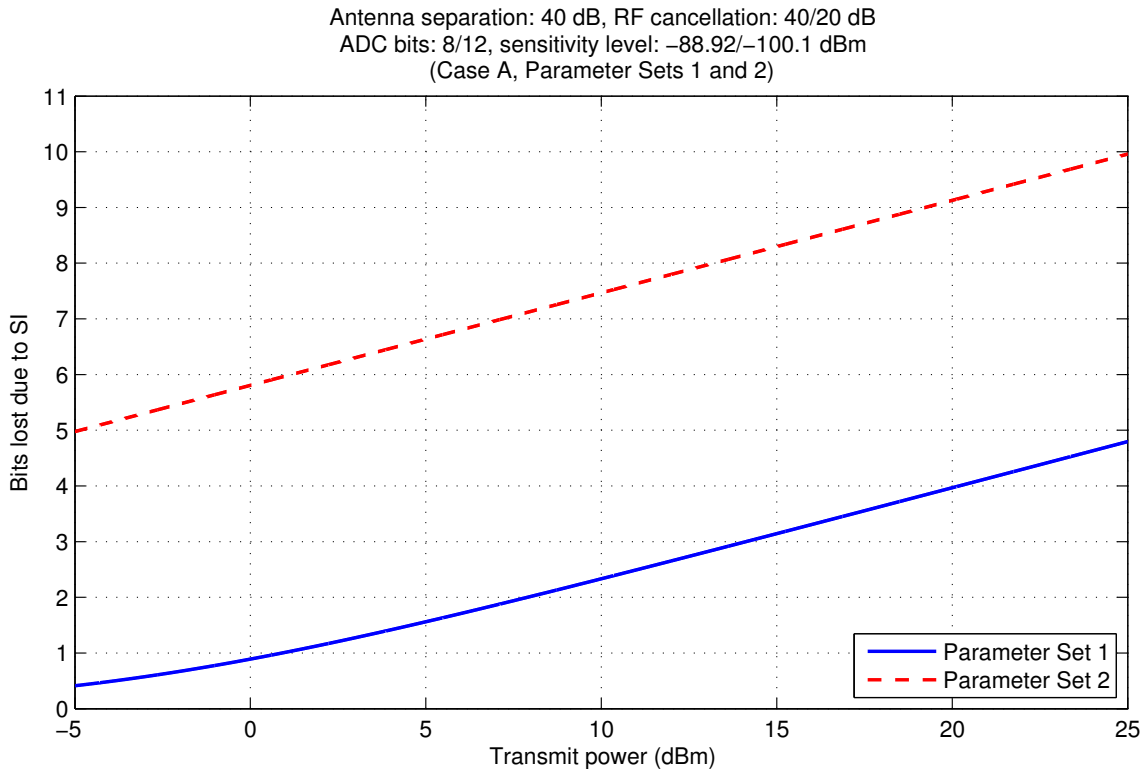

Figure 5.2: The amount of lost bits due to SI with both parameter sets.

To observe these factors in more detail, the amount of digital cancellation is next selected so that the loss of SINR caused by SI is fixed at 3 dB. This means that the combined power of the other distortion components is allowed to be equal to the power of the thermal noise included in the received signal. Thus, in this case, if the ratio between the signal of interest and dominating distortion becomes smaller than 15 dB, the above condition does not hold, and the loss of SINR becomes greater than 3 dB.

Below we provide closed-form solution for the required amount of digital cancellation. The linear SINR requirement, which must be fulfilled after digital cancellation, is denoted by $sinr_{\mathrm{RQ}}$. Then, the SINR requirement can only be fulfilled if

$$sinr_{\mathrm{RQ}} < \frac{g_{\mathrm{rx}} p_{\mathrm{SOI,in}}}{g_{\mathrm{rx}} F p_{\mathrm{N,in}} + p_{\mathrm{2nd}} + p_{\mathrm{3rd}} + \frac{g_{\mathrm{rx}} p_{\mathrm{3rd,PA,tx}}}{a_{\mathrm{ant}} a_{\mathrm{RF}}} + p_{\mathrm{quant}}}. \tag{5.1}$$

In words, this condition means that SINR must be above the minimum requirement without taking the SI into account. If the above condition is assumed to hold, the required SINR can be achieved with digital cancellation, and it can be written as

$$sinr_{\mathrm{RQ}} = \frac{g_{\mathrm{rx}} p_{\mathrm{SOI,in}}}{g_{\mathrm{rx}} F p_{\mathrm{N,in}} + \frac{g_{\mathrm{rx}}}{a_{\mathrm{ant}}} \left(\frac{p_{\mathrm{tx}}}{a_{\mathrm{RF}} a_{\mathrm{dig}}} + \frac{p_{\mathrm{3rd,PA,tx}}}{a_{\mathrm{RF}}} \right) + p_{\mathrm{2nd}} + p_{\mathrm{3rd}} + p_{\mathrm{quant}}}. \tag{5.2}$$

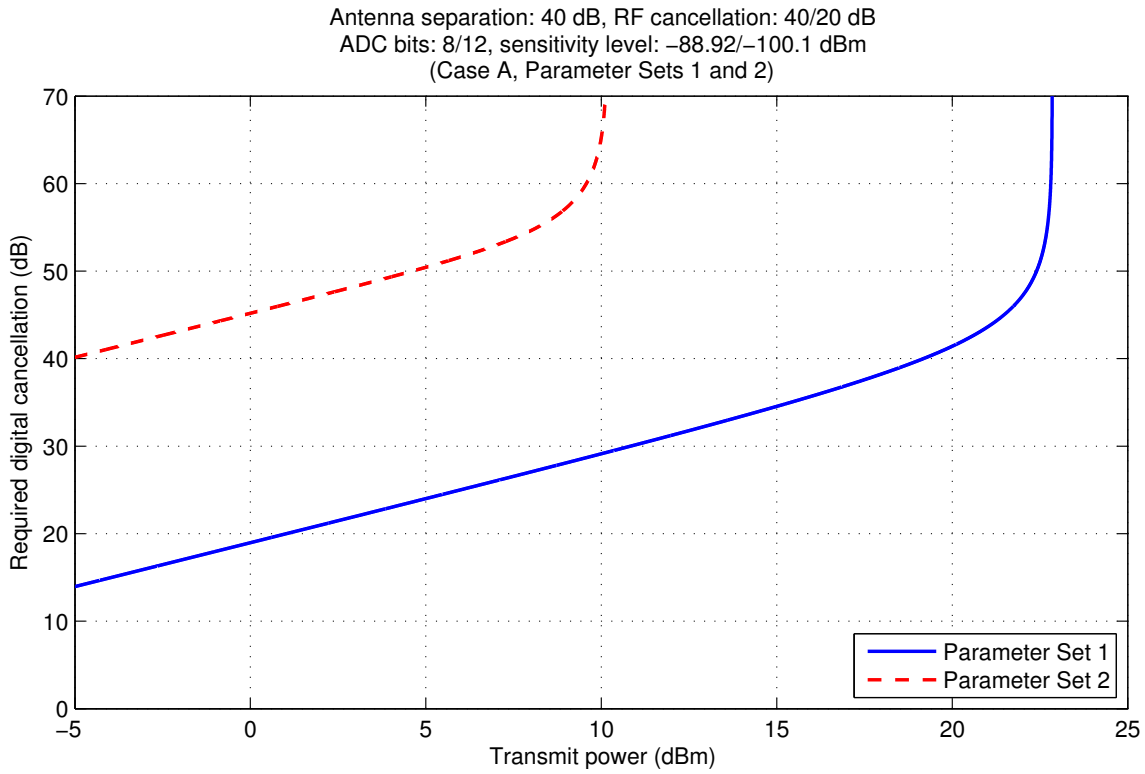

Figure 5.3: The required amount of digital cancellation to sustain a 3 dB SINR loss with both parameter sets.

From here, the amount of required digital cancellation can be derived and further modified into a compact form:

$$\begin{aligned} a_{\mathrm{dig}} &= \frac{\frac{g_{\mathrm{rx}} p_{\mathrm{tx}}}{a_{\mathrm{ant}} a_{\mathrm{RF}}}}{\frac{g_{\mathrm{rx}} p_{\mathrm{SOI,in}}}{sinr_{\mathrm{RQ}}} - (gF p_{\mathrm{N,in}} + p_{\mathrm{2nd}} + p_{\mathrm{3rd}} + \frac{g_{\mathrm{rx}} p_{\mathrm{3rd,PA,tx}}}{a_{\mathrm{ant}} a_{\mathrm{RF}}} + p_{\mathrm{quant}})} \\ &= \frac{1}{1 + \frac{a_{\mathrm{ant}} a_{\mathrm{RF}} p_{\mathrm{SOI,in}}}{p_{\mathrm{tx}}} \left(\frac{1}{sinr_{\mathrm{RQ}}} - \frac{1}{sinr_{\mathrm{DC}}} \right)}, \end{aligned} \tag{5.3}$$

where $sinr_{\mathrm{DC}}$ is the linear SINR before digital cancellation. The first form of the equation above shows that the amount of required digital cancellation is directly dependent on the transmit power. It can also be observed that increasing antenna separation or RF cancellation decreases the requirements for digital cancellation.

The required amount of digital cancellation to sustain 3 dB SINR loss, calculated from (5.3), is illustrated in Fig. 5.3. Again, the transmit power is varied from −5 dBm to 25 dBm and other parameters, apart from digital cancellation, are fixed. It can be observed that the maximum transmit power is approximately 23 dBm for Parameter Set 1. After this, the amount of needed digital cancellation increases to infinity, indicating perfect linear SI cancellation. However, as discussed earlier, after this point even perfect linear digital cancellation is not sufficient to maintain the required SINR as quantization noise and nonlinearities become the limiting factor.

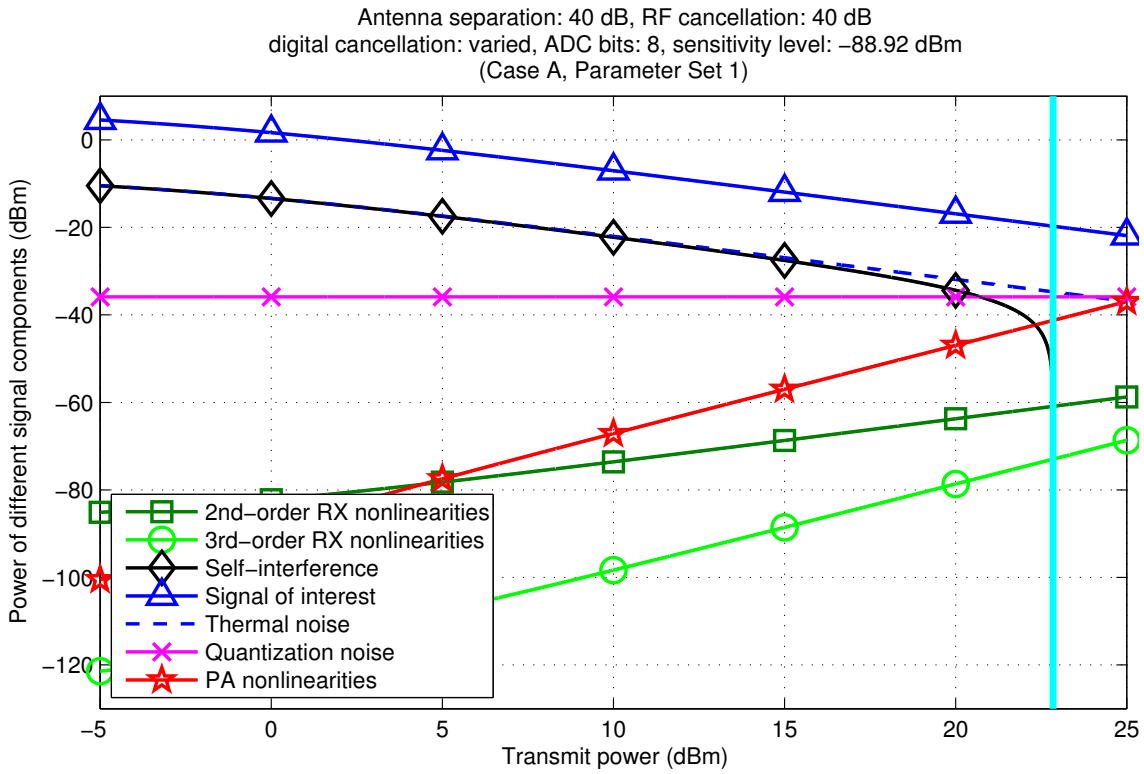

Figure 5.4: The power levels of different signal components at the input of the detector when the amount of digital cancellation is increased.

The power levels of the different signal components in this scenario are presented in Fig. 5.4. It can be observed that now quantization noise is the limiting factor for the SINR. The reason for this is that, with higher transmit powers and variable digital cancellation, the majority of SI is now cancelled in the digital domain and thus SI occupies almost completely the dynamic range of the ADC. This, on the other hand, deteriorates the resolution of the desired signal.

In order to further analyze the maximum transmit power of the considered full-duplex transceiver, it is next determined how it depends on different parameters. If the signal-to-(thermal)noise-ratio at the detector is marked by snr_d, the following equation holds when the loss of SINR is 3 dB:

$$snr_\mathrm{d} = \frac{g_\mathrm{rx} p_\mathrm{SOI,in}}{\frac{g_\mathrm{rx}}{a_\mathrm{ant}} \left(\frac{p_\mathrm{tx,max}}{a_\mathrm{RF} a_\mathrm{dig}} + \frac{p_\mathrm{3rd,PA,tx}}{a_\mathrm{RF}} \right) + p_\mathrm{2nd} + p_\mathrm{3rd} + p_\mathrm{quant}}. \tag{5.4}$$

This means that the power of the other types of distortion is equal to the power of thermal noise, resulting in a SINR loss of 3 dB.

When considering the maximum transmit power, it is assumed that digital SI cancellation is perfect. Furthermore, as the transmit power is high, and also the nonlinear distortion produced by the PA is attenuated by RF cancellation, the power of SI can be used to approximate the power of the total signal at the input of the

receiver chain. This, on the other hand, allows us to use (4.10) to approximate the total receiver gain with very small error. Thus, substituting g_{rx} in (5.4) with (4.10), letting $a_{\text{dig}} \to \infty$, and expressing quantization noise as $\frac{p_{\text{target}}}{snr_{\text{ADC}}}$, (5.4) becomes

$$\begin{aligned} snr_{\text{d}} &= \frac{\frac{a_{\text{ant}} a_{\text{RF}} p_{\text{target}}}{p_{\text{tx,max}}} p_{\text{SOI,in}}}{\frac{a_{\text{ant}} a_{\text{RF}} p_{\text{target}}}{p_{\text{tx,max}}} \frac{p_{\text{3rd,PA,tx}}}{a_{\text{ant}} a_{\text{RF}}} + p_{\text{2nd}} + p_{\text{3rd}} + \frac{p_{\text{target}}}{snr_{\text{ADC}}}} \\ &= \frac{a_{\text{ant}} a_{\text{RF}} p_{\text{SOI,in}}}{\frac{p_{\text{tx,max}}}{p_{\text{target}}} (p_{\text{2nd}} + p_{\text{3rd}}) + p_{\text{3rd,PA,tx}} + \frac{p_{\text{tx,max}}}{snr_{\text{ADC}}}} \\ &= \frac{a_{\text{ant}} a_{\text{RF}} p_{\text{SOI,in}}}{p_{\text{tx,max}} \left(\frac{p_{\text{2nd}} + p_{\text{3rd}}}{p_{\text{target}}} + \frac{1}{snr_{\text{ADC}}} \right) + p_{\text{3rd,PA,tx}}}. \end{aligned} \tag{5.5}$$

By solving (5.5) in terms of $p_{\text{tx,max}}$, the maximum transmit power can be calculated. However, as the power of nonlinear distortion is dependent on the transmit power, it is not convenient to derive an analytical equation for the maximum transmit power as it would require solving the roots of a 3rd-order polynomial.

However, if the scenario of Fig. 5.4 is considered, it can be seen that the quantization noise is actually the dominant distortion component. Thus, it can be written that $p_{\text{2nd}} + p_{\text{3rd}} \approx 0$ and $p_{\text{3rd,PA,tx}} \approx 0$, and in this case the maximum transmit power becomes

$$\begin{aligned} p_{\text{tx,max}} &= \frac{a_{\text{ant}} a_{\text{RF}} p_{\text{SOI,in}} snr_{\text{ADC}}}{snr_{\text{d}}}, \\ \text{i.e., } P_{\text{tx,max}} &= A_{\text{ant}} + A_{\text{RF}} + P_{\text{SOI,in}} + SNR_{\text{ADC}} - SNR_{\text{d}}. \end{aligned} \tag{5.6}$$

By substituting SNR_{ADC} with (4.6), the approximation of the maximum transmit power for the considered full-duplex transceiver can be written as

$$P_{\text{tx,max}} = A_{\text{ant}} + A_{\text{RF}} + P_{\text{SOI,in}} - SNR_{\text{d}} + 6.02b - PAPR + 4.76. \tag{5.7}$$

This applies accurately when the quantization noise is the limiting factor.

Yet another possible scenario is the situation, where the amount of bits is sufficiently high for the quantization noise to be negligibly low. In this case, the power of nonlinear distortion is the limiting factor for the maximum transmit power (still assuming $a_{\text{dig}} \to \infty$). In other words, if we let $snr_{\text{ADC}} \to \infty$, (5.5) becomes

$$snr_{\text{d}} = \frac{a_{\text{ant}} a_{\text{RF}} p_{\text{SOI,in}}}{p_{\text{tx,max}} \left(\frac{p_{\text{2nd}} + p_{\text{3rd}}}{p_{\text{target}}} \right) + p_{\text{3rd,PA,tx}}}. \tag{5.8}$$

However, similar to solving (5.5), it is again very inconvenient to derive a compact form for the maximum transmit power in this scenario, since it would again require solving the roots of a third order polynomial. Nevertheless, the value for the

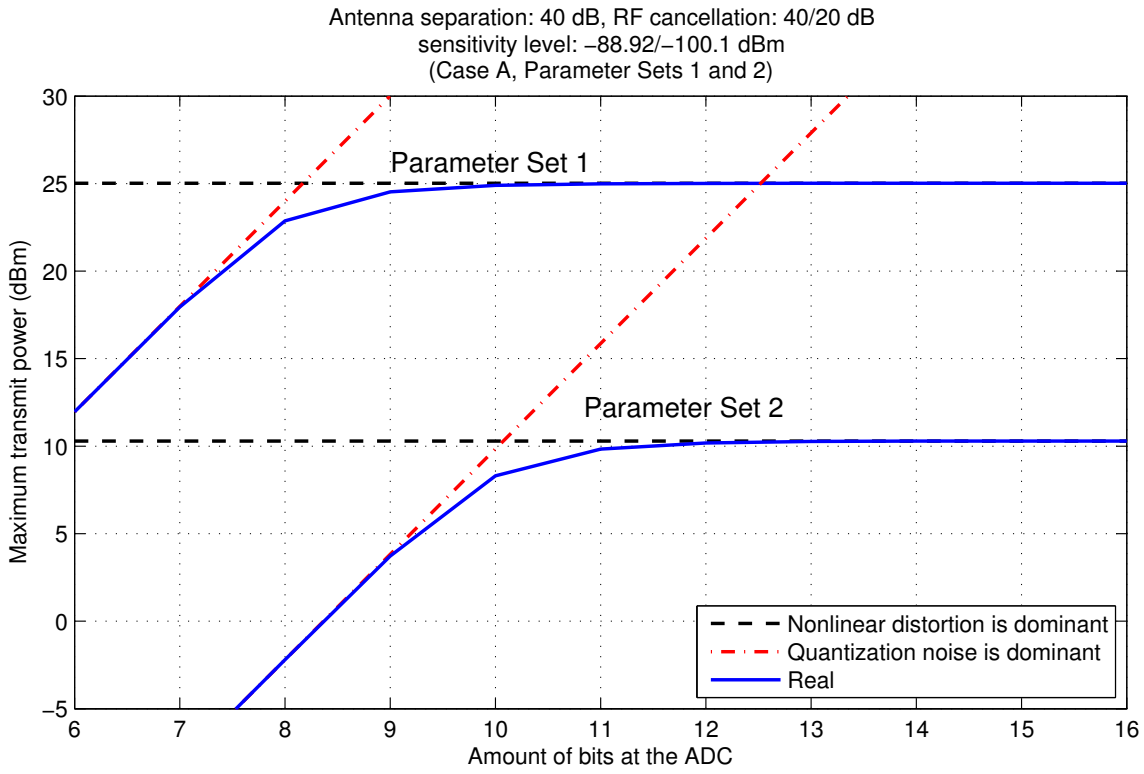

Figure 5.5: The maximum transmit power with respect to the number of bits at the ADC, again with both parameter sets. The solid curve shows the real value of the maximum transmit power, and the dash-dotted and dashed curves show the value when quantization noise or nonlinear distortion is the dominant distortion component, respectively.

maximum transmit power can in this case be easily calculated numerically, which yields $p_{\mathrm{tx,max}} \approx 25.02$ dBm and $p_{\mathrm{tx,max}} \approx 10.29$ dBm with Parameter Sets 1 and 2, respectively.

If operating under such conditions that neither intermodulation nor quantization noise is clearly dominating, previous results in (5.7) and (5.8) may be overestimating the performance. For this reason, Fig. 5.5 shows the actual maximum transmit power with respect to the number of bits at the ADC without any such assumptions, calculated numerically from (5.5). Also the maximum transmit powers for the two special scenarios are shown ($p_{\mathrm{2nd}} + p_{\mathrm{3rd}} \approx 0 / p_{\mathrm{3rd,PA,tx}} \approx 0$ and $snr_{\mathrm{ADC}} \to \infty$). With a low number of bits, the quantization noise is indeed the limiting factor for the transmit power and the curve corresponding to (5.7) is very close to the real value. On the other hand, with a high number of bits, the horizontal line corresponding to (5.8) is closer to the real value, as the power of quantization noise becomes negligibly low. This demonstrates very good accuracy and applicability of the derived analytical results.

Perhaps the most interesting observation from Fig. 5.5 is that with Parameter Set 1, it is sufficient to have a 10-bit ADC in order to decrease the power of quantization noise negligibly low. This is shown by the fact that after that point, the

maximum transmit power saturates to the value calculated with (5.8). The saturated value of the maximum transmit power can only be increased by selecting more linear transceiver components or by increasing the amount of SI attenuation in the analog domain, thereby decreasing the power of nonlinear distortion and thus lowering the overall noise floor.

Overall, with the chosen parameters for the receiver, the bottleneck during the full-duplex operation in Case A is the quantization noise, in addition to the actual SI. This is an observation worth noting, as performing as much SI cancellation in the digital domain as possible is very desirable, since it allows the construction of cheaper and more compact full-duplex transceivers with affordable and highly-integrated RF components. In addition, it is also observed that, with higher transmit powers, the nonlinear distortion produced by the PA of the transmitter is a considerable factor. If a cheaper and less linear PA is used, this nonlinear distortion starts to limit even more heavily the achievable performance of a full-duplex transceiver.

5.2.3 Calculations with Parameter Set 2

In order to analyze how using cheaper, and hence lower-quality, components affects the receiver chain, some calculations are done also with Parameter Set 2. The values of the parameters are listed in Tables 5.1 and 5.2. The sensitivity of the receiver is improved by decreasing the bandwidth and SNR requirement, and the power of the received signal is also decreased accordingly. In addition, the amount of RF cancellation is now assumed to be only 20 dB. This has a serious effect on the bit loss and the requirements for the digital cancellation.

The only component, whose specifications are improved, is the ADC, as it is now chosen to have 12 bits. The reason for this is to preserve sufficient resolution for the signal of interest in the digital domain, as the amount of lost bits is relatively high with these weaker parameters. The calculations are again carried out assuming that the amount of digital cancellation can be increased arbitrarily high.

The required amount of digital cancellation, when using Parameter Set 2, can be seen from Fig. 5.3, and Fig. 5.6 shows the power levels of the different signal components in this scenario, again calculated with (4.8)–(4.17). It can be seen that now nonlinear distortion, produced by the receiver components, is the limiting factor for the transmit power, instead of quantization noise. The maximum transmit power is only approximately 10 dBm. After this point, mitigating only the SI is not sufficient to sustain the required SINR, as nonlinear distortion decreases the SINR below the required level.

When observing the amount of lost bits from Fig. 5.2 with this parameter set, it can be seen that the bit loss is very high even with lower transmit powers. This is due to the decreased RF cancellation ability, which means that the SI power is

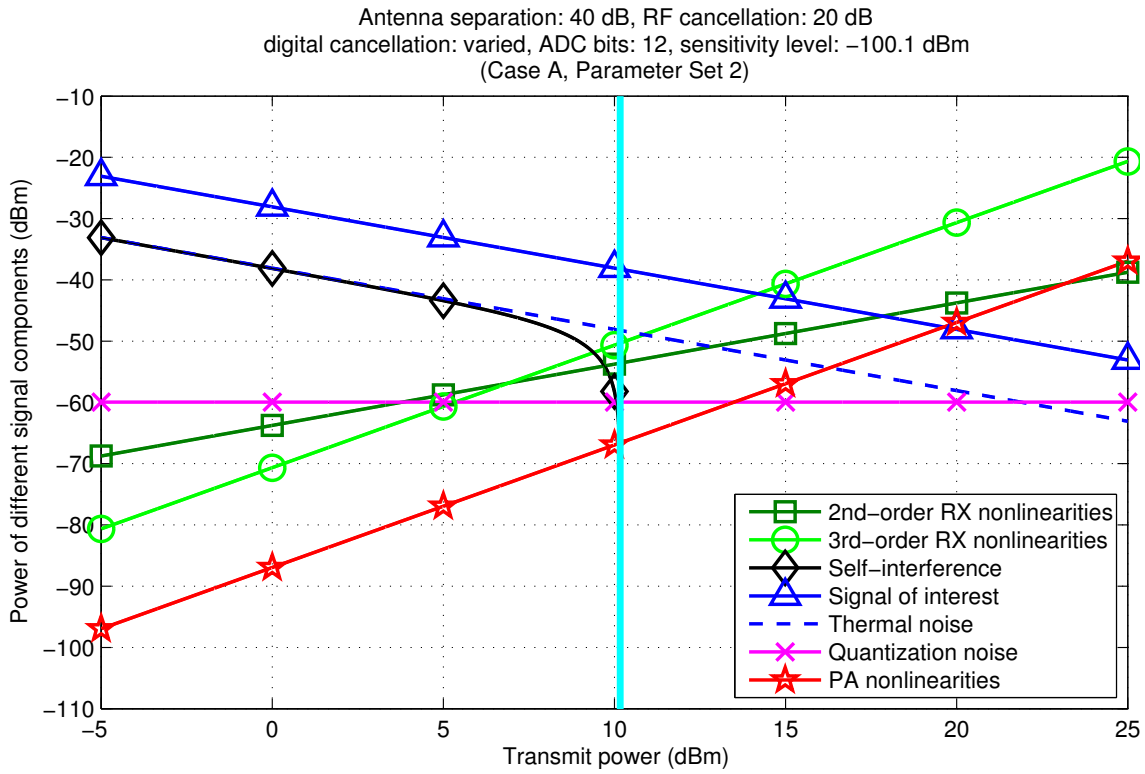

Figure 5.6: The power levels of different signal components with Parameter Set 2.

higher at the ADC interface. Thus, with lower SI cancellation performance at the analog/RF domain, the requirements for the ADC must be heavily increased in order to sustain reasonable resolution for the signal of interest.

It can also be concluded that, with cheaper and less linear components, mitigating the receiver chain nonlinearities might provide performance gain. This is shown by Fig. 5.5, where it can be observed that with Parameter Set 2, the maximum transmit power is decreased to 10 dBm, as opposed to the maximum transmit power of 25 dBm achieved with Parameter Set 1. This difference is caused by the lower linearity and decreased RF cancellation ability of the receiver utilizing Parameter Set 2. Thus, with decreased transceiver linearity and RF cancellation ability, also the RX-induced nonlinear distortion might have to be considered, as Figs. 5.5 and 5.6 demonstrate.

5.3 Results with Case B

In the system calculations of this section, Case B is considered, and thus the reference signal for RF cancellation is taken from the input of the PA. This means that the nonlinear distortion produced by the PA is not attenuated by RF cancellation, as it is not included in the cancellation signal. This will obviously increase the effect of these TX-induced nonlinearities. The values for the parameters of the RX chain are chosen according to Parameter Set 1, and the amount of digital cancellation is again controlled to maintain a 3 dB loss of SINR. The transmit power is varied from -5 dBm to 25 dBm.

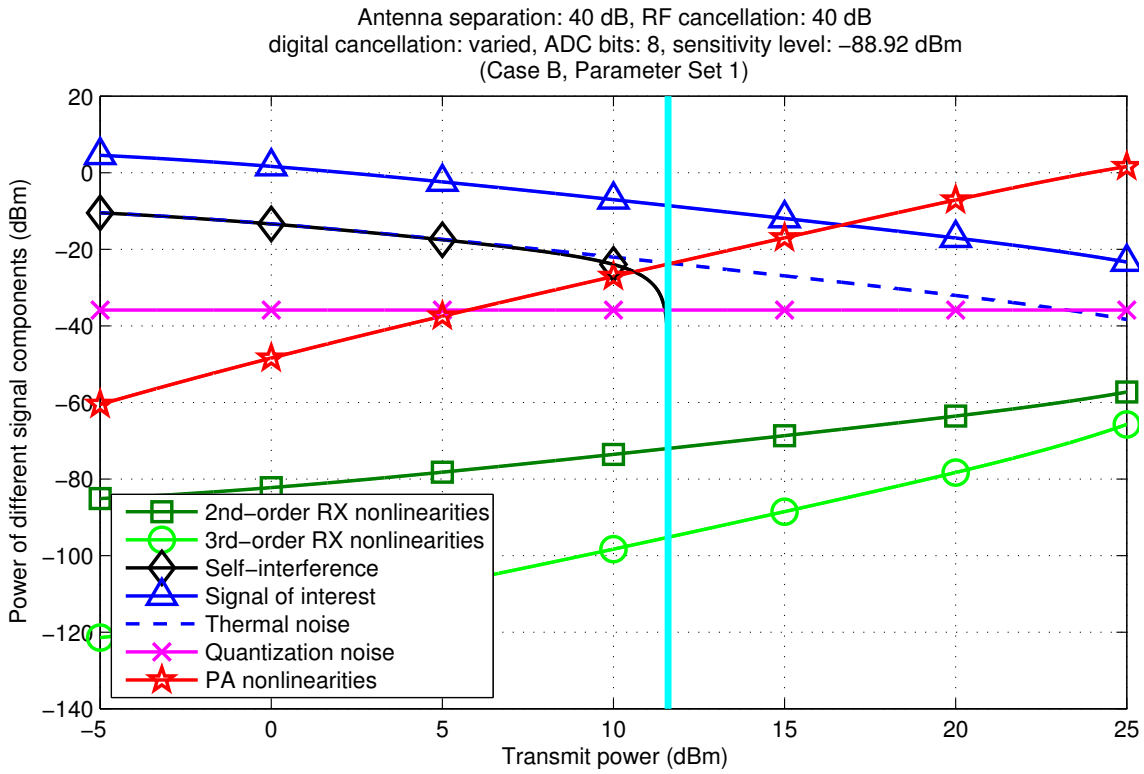

Figure 5.7: The power levels of the different signal components at the input of the detector, assuming Parameter Set 1 and Case B.

Figure 5.7 illustrates the power levels of different signal components in this scenario. It can be observed that the PA-induced nonlinear distortion is the most significant distortion component already with transmit powers higher than 11 dBm. Furthermore, with transmit powers higher than 12 dBm, it will decrease the SINR below the required level, thus preventing the usage of higher transmit powers.

When comparing Fig. 5.7 to Fig. 5.4, it can be observed that the difference is significant. This is caused by the fact that in Case B, the nonlinear distortion produced by the PA is not attenuated by RF cancellation, unlike in Case A. Hence, it is clear that ability to mitigate nonlinear distortion would provide significant performance gain for a full-duplex transceiver which is implemented according to Case B. Furthermore, with the chosen parameters, it would be sufficient to mitigate the nonlinearities in the digital domain, as the quantization noise floor is relatively low with respect to the other signal components.

In order to study the effect of nonlinear cancellation, the maximum transmit powers of two different cases are compared. In the first case, it is assumed that digital cancellation is linear, and can thus mitigate only the linear part of the SI signal. In the other case, it is assumed that digital cancellation is able to mitigate also the nonlinear part of the SI signal, in addition to the linear part. Figure 5.8 shows the increase in the maximum transmit power, when comparing these two

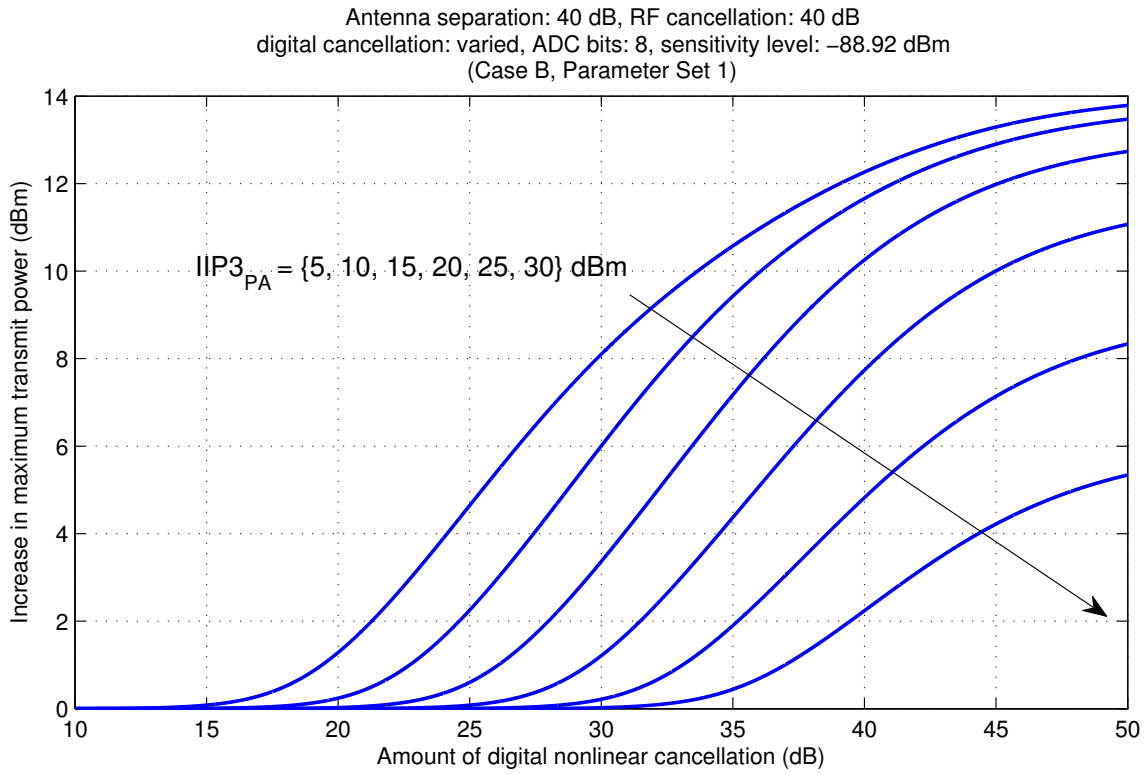

Figure 5.8: The increase in maximum transmit power when also the nonlinear distortion of the SI channel can be mitigated with digital cancellation, compared to only linear cancellation. Horizontal axis depicts the total amount of achieved digital cancellation. The curves correspond to different IIP3 figures of the PA.

scenarios. The same curve has been plotted with different IIP3 values for the PA. The curves have been calculated based on (4.8)–(4.17), with the modification that in the other case, $P_{\mathrm{3rd,PA}}$ is also attenuated by A_{dig}. It can be observed that being able to mitigate the nonlinear component of the SI signal in the digital domain provides a significant increase in the maximum transmit power when the total amount of digital cancellation is increased. This has also been observed with actual waveform simulations in [12].

It can also be observed that already with 25 dB of digital cancellation, the maximum transmit power is increased by as much as 5 dB, if also the nonlinear component of the SI signal is mitigated. Obviously, the achievable gain is smaller with a more linear PA, and this indicates that when the nonlinear component of the SI signal is weaker, linear digital cancellation might be sufficient. However, with a less linear PA, significant increase in the maximum transmit power can be achieved with nonlinear digital cancellation, almost regardless of the total amount of achieved cancellation.

Overall, Figures 5.7 and 5.8 illustrate that nonlinear distortion produced by the transmitter PA is a significant issue in full-duplex transceivers, when the reference signal for RF cancellation is taken from the input of the PA. Furthermore, the ability to attenuate it can significantly improve the performance of the transceiver.

6. WAVEFORM SIMULATIONS

In order to analyze and demonstrate the good accuracy of the used models and the system level calculation results, a complete full-duplex waveform simulator is constructed. It emulates a similar direct-conversion transceiver that is used in the analytical calculations. However, for brevity, only Case A with Parameter Set 1 is considered as it is sufficient to use only this one case to obtain a reliable comparison between analytical calculations and waveform simulations.

6.1 Simulator overview

The simulator is implemented with Matlab and Simulink, using SimRF component library. The Simulink model is shown in Fig. 6.1, and it simulates the analog portion of the transceiver chain. The simulated waveform is chosen to be an OFDM signal with parameters specified in Table 6.1. The parameters are in essence similar to WLAN specifications, and they are used for generating all the signals.

The SI channel is assumed to be static and it consists of a main coupling component and three weak multipath components, delayed by one, three, and eight sample intervals in relation to the main component, respectively. This corresponds to a maximum delay of 125 ns. The delay of the main component is assumed to be negligibly small, as the distance between the antennas is typically very short. The average power difference between the main component and the multipath components is set to 45 dB, which is on the same range as values measured in [26].

In the simulations, RF cancellation attenuates only the main component of the SI signal, corresponding to the considered full-duplex transceiver model. Also some delay, amplitude, and phase errors are included in the RF cancellation signal to achieve the desired amount of SI attenuation, and to model the cancellation process in a realistic manner.

The attenuation of the weaker multipath components is then done by digital cancellation after the ADC. The implementation of digital cancellation utilizes classic least-squares based SI coupling channel estimation, which is implemented with linear least-squares fitting between the ideal TX data and RX observation during a calibration period. Thus, the amount of digital cancellation cannot be tuned arbitrarily since it depends directly on the accuracy of these TX-RX channel estimates. The amount of achieved digital cancellation is illustrated in Fig. 6.2. The fluctuating curve is the realized value, and the smooth curve is a third order polynomial fitted to

Table 6.1: Additional parameters for the waveform simulator.

Parameter	Value
Constellation	16-QAM
Number of subcarriers	64
Number of data subcarriers	48
Guard interval	16 samples
Sample length	15.625 ns
Symbol length	4 μs
Signal bandwidth	12.5 MHz
Oversampling factor	4

the realized values. The polynomial approximation is used when calculating the analytical SINR, in order to assess realistic average performance. As shown in Fig. 6.2, large amount of cancellation is achieved with higher transmit powers, as the quality of the channel estimate is better with a stronger SI signal. This phenomenon has also been observed in practice [26]. However, with transmit powers above 17 dBm, the power of the PA-induced nonlinear distortion starts to decrease the achievable digital cancellation.

6.2 Comparison to analytical calculations

The results of the analytical calculations are compared to the simulation results in terms of the SINR at the input of the detector ($SINR_{\mathrm{d}}$). In the waveform simulator, the SINR is calculated by first determining the effective powers for the ideal signal, and total noise-plus-interference signal. After this, the SINR is calculated as the ratio of these signal powers. The simulation is repeated 50 times for each transmit power, and the transmit power is varied with 1 dB intervals. The SINR corresponding to each transmit power is calculated as the average value of these independent realizations. The analytical SINR is calculated directly from the previously presented equations.

Figure 6.3 shows the SINRs obtained with analytical calculations and with full waveform simulations, with respect to transmit power. It can be seen that the two curves are practically identical, thus evidencing excellent accuracy and reliability of the reported analytical expressions. With closer inspection, it can be observed that the analytically calculated SINR is actually slightly pessimistic throughout the considered transmit power range, but the difference is only in the order of 0.1–0.3 dB. This is likely to be caused by the different approximations made when deriving the equations for the power levels of the different signal components. In any case, it can be concluded that the accuracy of the analysis is very high.

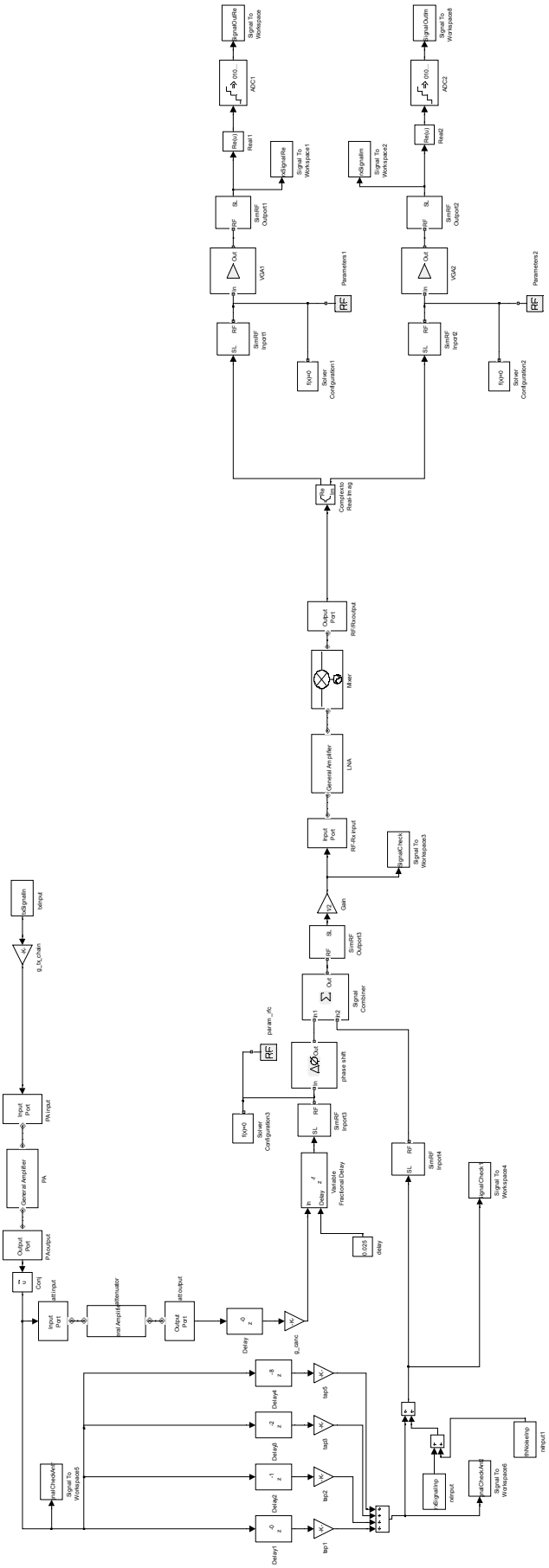

Figure 6.1: The Simulink model of the waveform simulator.

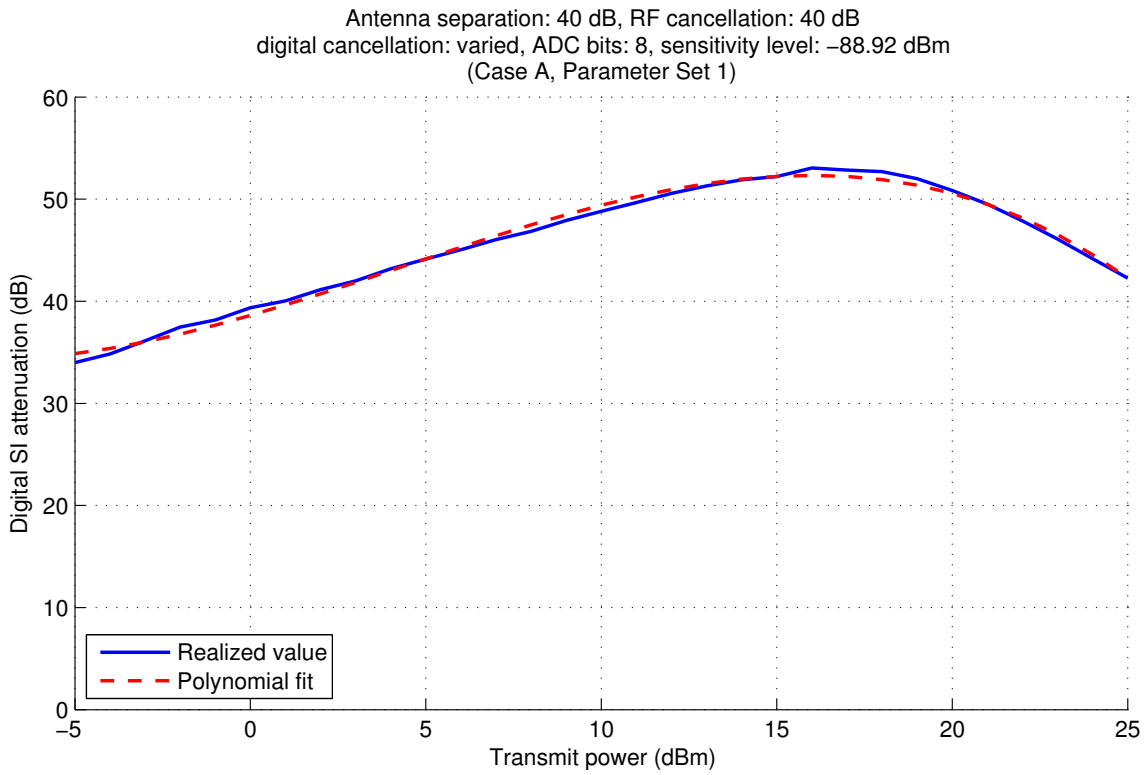

Figure 6.2: The amount of achieved digital cancellation in the waveform simulations, with respect to transmit power.

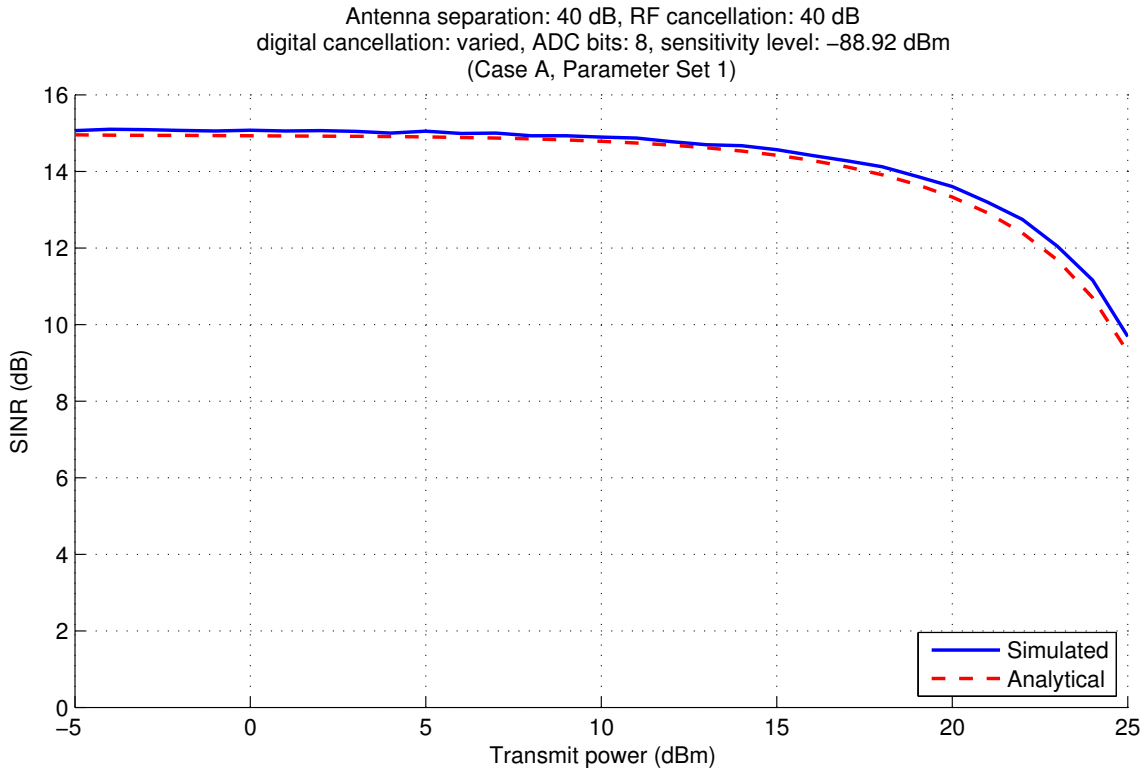

Figure 6.3: SINR values obtained from the waveform simulations and from the analytical calculations.

7. CONCLUSION

In this thesis, the effect of self-interference on the receiver chain of a full-duplex transceiver was analyzed for two slightly different implementations. This analysis is needed in order to obtain information regarding the magnitude of various nonidealities occurring in the different components of the transceiver chain. The parameters used in the modeling of the transceiver are largely based on practical full-duplex implementations and real transceiver implementations.

The calculations showed that if the reference signal for RF cancellation is taken from the output of the transmitter's power amplifier, quantization noise at the receiver's analog-to-digital converter is typically the most significant problem. This is caused by the strong self-interference, which reserves most of the dynamic range. It was also observed that, with less linear components and with increased transmit power, the intermodulation of the transmitter power amplifier and receiver components, causing nonlinear self-interference, can become a limiting factor for the receiver performance. In particular, if the linearity of the receiver chain is not sufficiently high, the receiver amplifiers will introduce significantly powerful nonlinear distortion into the the self-interference signal when using higher transmit powers.

In another scenario, where the reference for RF cancellation is taken from the input of the power amplifier, it was observed that the nonlinear distortion of the self-interference signal becomes the most significant distortion component with even lower transmit powers. Thus, when using this type of an implementation, the linearity of the power amplifier is one of the main bottlenecks of a full-duplex transceiver.

The reliability of the results obtained from the calculations was demonstrated by their similarity with the results acquired from complete waveform simulations. This indicates that it is sufficient to use the derived equations in the dimensioning of a full-duplex transceiver. In addition, although the purpose of the simulations in this thesis was to merely confirm the accuracy of the analytical models, the developed waveform simulator is an useful tool also for future work on single-channel full-duplex communications.

Altogether, the results of this thesis demonstrate a need for high number of bits in the analog-to-digital converter or, alternatively, a significant amount of self-interference cancellation in the analog domain. It is also shown that there is a need to address the RF impairments, especially power amplifier nonlinearity, and possi-

bly also the nonlinearity of the receiver components, in baseband self-interference cancellation. The other option would be to use more expensive, highly linear amplifiers. However, in the context of commercial radio devices, it is more feasible to opt for cheaper and less linear components, and use digital signal processing algorithms to counteract the non-idealities. Thus, the effect of quantization in the analog-to-digital conversion and nonlinearity of the transceiver chain should always be taken into account when implementing a full-duplex transceiver, as they have a significant effect on its final performance.

7.1 Future work

One potential topic for future work is the development of nonlinear baseband self-interference cancellation methods. The need for these methods is demonstrated by the results of this thesis, as nonlinear distortion proved to be a significant bottleneck in several situations. Thus, to facilitate transmit powers anywhere near the typical WiFi or cellular device range, also the nonlinear self-interference must be attenuated by some means. Extending these cancellation techniques to full-duplex MIMO architectures is also one possible future step in the research on single channel full-duplex communications.

As another topic for future work, one could analyze how the amount of self-interference cancellation occurring before analog-to-digital conversion could be increased. One possible method for this would be analog baseband cancellation, where the digital cancellation signal is fed to the input of the analog-to-digital converters via additional digital-to-analog converters. Using this method, the filtering of the cancellation signal could be done in the digital domain, which is significantly more convenient than performing the same operations with analog circuitry. In addition, under rapidly changing channel conditions, the adaptation of the filter coefficients can be done more efficiently in the digital domain. Employing an additional analog self-interference cancellation stage would decrease the power of the self-interference signal in the analog domain, and thus also decrease the effect of quantization noise. Furthermore, it would require only two additional digital-to-analog converters, thus being a relatively cheap option in contrast to earlier concepts that assign a complete transmitter chain for digital-to-analog cancellation.

BIBLIOGRAPHY

[1] LTE; evolved universal terrestrial radio access (E-UTRA); user equipment (UE) radio transmission and reception (3GPP TS 36.101 version 11.2.0 release 11). ETSI, Sophia Antipolis Cedex, France.

[2] QHx-220 active isolation enhancer and interference canceller. Intersil, Milpitas, California, USA.

[3] TLV1548-Q1 Low-voltage 10-bit analog-to-digital converter with serial control and 8 analog inputs. Texas Instruments, Dallas, Texas, USA.

[4] Universal mobile telecommunications system (UMTS); UTRAN architecture for 3G home node B (HNB); stage 2 (3GPP TS 25.467 version 11.4.0 release 11). ETSI, Sophia Antipolis Cedex, France.

[5] V. Aggarwal, M. Duarte, A. Sabharwal, and N.K. Shankaranarayanan. Full- or half-duplex? a capacity analysis with bounded radio resources. In *Proc. Information Theory Workshop (ITW)*, pages 207–211, 2012.

[6] E. Ahmed, A. Eltawil, and A. Sabharwal. Simultaneous transmit and sense for cognitive radios using full-duplex: A first study. In *Proc. Antennas and Propagation Society International Symposium (APSURSI)*, pages 1–2, 2012.

[7] E. Ahmed, A. Eltawil, and A. Sabharwal. Rate gain region and design tradeoffs for full-duplex wireless communications. *IEEE Transactions on Wireless Communications*, 12(7):3556–3565, 2013.

[8] E. Ahmed, A. Eltawil, and A. Sabharwal. Self-interference cancellation with nonlinear distortion suppression for full-duplex systems. In *Proc. 47th Asilomar Conference on Signals, Systems and Computers*, 2013.

[9] E. Ahmed, A. Eltawil, and A. Sabharwal. Self-interference cancellation with phase noise induced ICI suppression for full-duplex systems. *CoRR*, abs/1307.4149, 2013.

[10] I. Akyildiz, W. Lee, M. Vuran, and S. Mohanty. Next generation/dynamic spectrum access/cognitive radio wireless networks: A survey. *Computer Networks*, 50(13):2127–2159, 2006.

[11] E. Antonio-Rodriguez and R. Lopez-Valcarce. Adaptive self-interference suppression for full-duplex relays with multiple receive antennas. In *Proc. 13th International Workshop on Signal Processing Advances in Wireless Communications (SPAWC)*, pages 454–458, 2012.

[12] L. Anttila, D. Korpi, V. Syrjälä, and M. Valkama. Cancellation of power amplifier induced nonlinear self-interference in full-duplex transceivers. In *Proc. 47th Asilomar Conference on Signals, Systems and Computers*, 2013.

[13] E. Aryafar, M. Khojastepour, K. Sundaresan, S. Rangarajan, and M. Chiang. MIDU: enabling MIMO full duplex. In *Proc. 18th annual international conference on Mobile computing and networking*, pages 257–268, New York, NY, USA, 2012. ACM.

[14] A. Behzad. *Wireless LAN Radios: System Definition to Transistor Design*. IEEE Series on Digital and Mobile Communication. Wiley, 2007.

[15] D. Bharadia, E. McMilin, and S. Katti. Full duplex radios. In *Proc. SIGCOMM'13*, Hong Kong, China, August 2013.

[16] D.W. Bliss, P.A. Parker, and A.R. Margetts. Simultaneous transmission and reception for improved wireless network performance. In *Proc. 14th Workshop on Statistical Signal Processing*, pages 478–482, 2007.

[17] S. Chen, M.A. Beach, and null. Division-free duplex for wireless applications. *Electronics Letters*, 34(2):147–148, 1998.

[18] W. Cheng, X. Zhang, and H. Zhang. Full duplex spectrum sensing in non-time-slotted cognitive radio networks. In *Military Communications Conference (MILCOM)*, pages 1029–1034, 2011.

[19] W. Cheng, X. Zhang, and H. Zhang. QoS driven power allocation over full-duplex wireless links. In *Proc. IEEE International Conference on Communications (ICC)*, pages 5286–5290, 2012.

[20] J. I. Choi, M. Jain, K. Srinivasan, P. Levis, and S. Katti. Achieving single channel full duplex wireless communication. In *Proc. 16th Annual International Conference on Mobile Computing and Networking*, MobiCom '10, pages 1–12, New York, NY, USA, 2010. ACM.

[21] Y. Choi and H. Shirani-Mehr. Simultaneous transmission and reception: Algorithm, design and system level performance, 2013.

[22] B. Chun and H. Park. A spatial-domain joint-nulling method of self-interference in full-duplex relays. *IEEE Communications Letters*, 16(4):436–438, 2012.

[23] C. Cox and E. Ackerman. Demonstration of a single-aperture, full-duplex communication system. In *Proc. Radio and Wireless Symposium*, pages 148–150, 2013.

[24] B.P. Day, A.R. Margetts, D.W. Bliss, and P. Schniter. Full-duplex bidirectional MIMO: Achievable rates under limited dynamic range. *IEEE Transactions on Signal Processing*, 60(7):3702–3713, 2012.

[25] B.P. Day, A.R. Margetts, D.W. Bliss, and P. Schniter. Full-duplex MIMO relaying: Achievable rates under limited dynamic range. *IEEE Journal on Selected Areas in Communications*, 30(8):1541–1553, 2012.

[26] M. Duarte, C. Dick, and A. Sabharwal. Experiment-driven characterization of full-duplex wireless systems. *IEEE Transactions on Wireless Communications*, 11(12):4296 –4307, December 2012.

[27] M. Duarte and A. Sabharwal. Full-duplex wireless communications using off-the-shelf radios: Feasibility and first results. In *Proc. 44th Asilomar Conference on Signals, Systems, and Computers*, November 2010.

[28] E. Everett, M. Duarte, C. Dick, and A. Sabharwal. Empowering full-duplex wireless communication by exploiting directional diversity. In *Proc. 45th Asilomar Conference on Signals, Systems and Computers*, pages 2002–2006, 2011.

[29] Q. Gu. *RF System Design of Transceivers for Wireless Communications*. Springer-Verlag New York, Inc., Secaucus, NJ, USA, 2006.

[30] D. Halperin, T. Anderson, and D. Wetherall. Taking the sting out of carrier sense: interference cancellation for wireless LANs. In *Proc. 14th ACM international conference on Mobile computing and networking*, pages 339–350, New York, NY, USA, 2008. ACM.

[31] M. Jain, J. I. Choi, T. Kim, D. Bharadia, S. Seth, K. Srinivasan, P. Levis, S. Katti, and P. Sinha. Practical, real-time, full duplex wireless. In *Proc. 17th Annual International Conference on Mobile Computing and Networking*, MobiCom '11, pages 301–312, New York, NY, USA, 2011. ACM.

[32] H. Jin and V.C.M. Leung. Full-duplex transmissions in fiber-connected distributed relay antenna systems. In *Proc. Global Communications Conference (GLOBECOM)*, pages 4284–4289, 2012.

[33] A. Katz. Linearization: reducing distortion in power amplifiers. *IEEE Microwave Magazine*, 2(4):37–49, 2001.

[34] M.A. Khojastepour and S. Rangarajan. Wideband digital cancellation for full-duplex communications. In *Proc. 46th Asilomar Conference on Signals, Systems and Computers*, pages 1300–1304, 2012.

[35] C. Kim, E. Jeong, Y. Sung, and Y. H. Lee. Asymmetric complex signaling for full-duplex decode-and-forward relay channels. In *Proc. International Conference on ICT Convergence (ICTC)*, pages 28–29, 2012.

[36] H. Kim, S. Lim, H. Wang, and D. Hong. Power allocation and outage probability analysis for secondary users in cognitive full duplex relay systems. In *Proc. 13th International Workshop on Signal Processing Advances in Wireless Communications (SPAWC)*, pages 449–453, 2012.

[37] M. E. Knox. Single antenna full duplex communications using a common carrier. In *Proc. 13th Annual Wireless and Microwave Technology Conference (WAMICON)*, pages 1 –6, April 2012.

[38] D. Korpi, L. Anttila, V. Syrjälä, and M. Valkama. Widely-linear digital self-interference cancellation in direct-conversion full-duplex transceiver. *Submitted and under peer-review*, to be published, 2014.

[39] D. Korpi, T. Riihonen, V. Syrjälä, L. Anttila, M. Valkama, and R. Wichman. Full-duplex transceiver system calculations: Analysis of ADC and linearity challenges. *Submitted and under peer-review*, to be published, 2014.

[40] D. Korpi, M. Valkama, T. Riihonen, and R. Wichman. Implementation challenges in full-duplex radio transceiver. In *Proc. XXXIII Finnish URSI Convention on Radio Science*, Espoo, Finland, April 2013.

[41] D. Korpi, S. Venkatasubramanian, T. Riihonen, L. Anttila, S. Otewa, C. Icheln, K. Haneda, S. Tretyakov, M. Valkama, and R. Wichman. Advanced self-interference cancellation and multiantenna techniques for full-duplex radios. In *Proc. 47th Asilomar Conference on Signals, Systems and Computers*, 2013.

[42] Shenghong L. and R.D. Murch. Full-duplex wireless communication using transmitter output based echo cancellation. In *Proc. Global Telecommunications Conference (GLOBECOM 2011)*, pages 1–5, 2011.

[43] Jong-Ho Lee and Oh-Soon Shin. Distributed beamforming approach to full-duplex relay in multiuser MIMO transmission. In *Proc. Wireless Communications and Networking Conference Workshops (WCNCW)*, pages 278–282, 2012.

[44] P. Lioliou, M. Viberg, M. Coldrey, and F. Athley. Self-interference suppression in full-duplex MIMO relays. In *Proc. 44th Asilomar Conference on Signals, Systems and Computers*, pages 658–662, 2010.

[45] J.G. McMichael and K.E. Kolodziej. Optimal tuning of analog self-interference cancellers for full-duplex wireless communication. In *Proc. 50th Annual Allerton Conference on Communication, Control, and Computing*, pages 246–251, 2012.

[46] K. Miura and M. Bandai. Node architecture and MAC protocol for full duplex wireless and directional antennas. In *Proc. 23rd International Symposium on Personal Indoor and Mobile Radio Communications (PIMRC)*, pages 369–374, 2012.

[47] A. Pärssinen, J. Jussila, J. Ryynänen, L. Sumanen, and K. A. I. Halonen. A 2-GHz wide-band direct conversion receiver for WCDMA applications. *IEEE Journal of Solid-State Circuits*, 34(12):1893–1903, December 1999.

[48] N. Phungamngern, P. Uthansakul, and M. Uthansakul. Digital and rf interference cancellation for single-channel full-duplex transceiver using a single antenna. In *Proc. 10th International Conference on Electrical Engineering/Electronics, Computer, Telecommunications and Information Technology (ECTI-CON)*, pages 1–5, 2013.

[49] F.H. Raab, P. Asbeck, S. Cripps, P.B. Kenington, Z.B. Popovic, N. Pothecary, J.F. Sevic, and N.O. Sokal. Power amplifiers and transmitters for RF and microwave. *IEEE Transactions on Microwave Theory and Techniques*, 50(3):814–826, 2002.

[50] B. Radunovic, D. Gunawardena, P. Key, A. Proutiere, N. Singh, V. Balan, and G. DeJean. Rethinking indoor wireless mesh design: Low power, low frequency, full-duplex. In *Proc. Fifth IEEE Workshop on Wireless Mesh Networks (WIMESH 2010)*, pages 1–6, 2010.

[51] B. Razavi. *RF microelectronics*. Prentice Hall communications engineering and emerging technologies series. Prentice-Hall, Inc., Upper Saddle River, NJ, USA, 1998.

[52] T. Riihonen, P. Mathecken, and R. Wichman. Effect of oscillator phase noise and processing delay in full-duplex OFDM repeaters. In *Proc. 46th Asilomar Conference on Signals, Systems and Computers*, pages 1947–1951, 2012.

[53] T. Riihonen, M. Vehkapera, and R. Wichman. Large-system analysis of rate regions in bidirectional full-duplex mimo link: Suppression versus cancellation. In *Proc. 47th Annual Conference on Information Sciences and Systems (CISS)*, pages 1–6, 2013.

[54] T. Riihonen, S. Werner, J.E. Cousseau, and R. Wichman. Design of co-phasing allpass filters for full-duplex OFDM relays. In *Proc. 42nd Asilomar Conference on Signals, Systems and Computers*, pages 1030–1034, 2008.

[55] T. Riihonen, S. Werner, and R. Wichman. Comparison of full-duplex and half-duplex modes with a fixed amplify-and-forward relay. In *Proc. Wireless Communications and Networking Conference*, pages 1–5, 2009.

[56] T. Riihonen, S. Werner, and R. Wichman. Optimized gain control for single-frequency relaying with loop interference. *IEEE Transactions on Wireless Communications*, 8(6):2801–2806, 2009.

[57] T. Riihonen, S. Werner, and R. Wichman. Hybrid full-duplex/half-duplex relaying with transmit power adaptation. *IEEE Transactions on Wireless Communications*, 10(9):3074–3085, 2011.

[58] T. Riihonen, S. Werner, and R. Wichman. Mitigation of loopback self-interference in full-duplex MIMO relays. *IEEE Transactions on Signal Processing*, 59(12):5983–5993, 2011.

[59] T. Riihonen and R. Wichman. Analog and digital self-interference cancellation in full-duplex MIMO-OFDM transceivers with limited resolution in A/D conversion. In *Proc. 46th Asilomar Conference on Signals, Systems and Computers*, pages 45–49, 2012.

[60] A. Sabharwal. New results in multiuser full-duplex. In *Proc. 47th Asilomar Conference on Signals, Systems and Computers*, 2013.

[61] A. Sahai, G. Patel, C. Dick, and A. Sabharwal. Understanding the impact of phase noise on active cancellation in wireless full-duplex. In *Proc. 46th Asilomar Conference on Signals, Systems and Computers*, pages 29–33, 2012.

[62] A. Sahai, G. Patel, and A. Sabharwal. Pushing the limits of full-duplex: Design and real-time implementation. Technical Report TREE1104, Department of Electrical and Computer Engineering, Rice University, July 2011.

[63] A. Sahai, G. Patel, and A. Sabharwal. Asynchronous full-duplex wireless. In *Proc. Fourth International Conference on Communication Systems and Networks (COMSNETS)*, pages 1–9, 2012.

[64] D. Senaratne and C. Tellambura. Beamforming for space division duplexing. In *Proc. IEEE International Conference on Communications (ICC)*, pages 1–5, 2011.

[65] C. E. Shannon. A mathematical theory of communication. *Bell System Technical Journal*, 27, 1948.

[66] N. Shende, O. Gurbuz, and E. Erkip. Half-Duplex or Full-Duplex Relaying: A Capacity Analysis under Self-Interference. *ArXiv e-prints*, March 2013.

[67] Young-Keum Song and Dongwoo Kim. Convergence of distributed power control with full-duplex amplify-and-forward relays. In *Proc. International Conference on Wireless Communications Signal Processing*, pages 1–5, 2009.

[68] V. Syrjälä, M. Valkama, L. Anttila, T. Riihonen, and D. Korpi. Analysis of oscillator phase-noise effects on self-interference cancellation in full-duplex OFDM radio transceivers. *Accepted for publication in IEEE Transactions on Wireless Communications*, 2014.

[69] H. Yoo, K. Woo, C. Park, J. Kim, S. Jung, and Y. Cho. A synchronization technique for frequency-domain feedback interference canceller in OFDM-based full duplex relays. In *Proc. 70th Vehicular Technology Conference Fall (VTC 2009-Fall)*, pages 1–5, 2009.

[70] H. Yoshida, T. Kato, T. Toyoda, I. Seto, R. Fujimoto, T. Kimura, O. Watanabe, T. Arai, T. Itakura, and H. Tsurumi. Fully differential direct conversion receiver for W-CDMA using an active harmonic mixer. In *Proc. Radio Frequency Integrated Circuits (RFIC) Symposium*, pages 395–398, June 2003.

[71] J. Zhang, L. Fu, and X. Wang. Asymptotic analysis on secrecy capacity in large-scale wireless networks, 2013.

[72] G. Zheng, I. Krikidis, J. Li, A.P. Petropulu, and B. Ottersten. Improving physical layer secrecy using full-duplex jamming receivers. *IEEE Transactions on Signal Processing*, 61(20):4962–4974, 2013.

[73] G. Zheng, I. Krikidis, and B. Ottersten. Full-duplex cooperative cognitive radio with transmit imperfections, 2013.

A. DERIVATIONS OF RECEIVER NONLINEAR DISTORTION PRODUCTS

The derivation of (4.14) and (4.15) is done based on the power of nonlinear distortion at the output of a single component. This, on the other hand, can be calculated with (4.7). In the considered full-duplex transceiver, only the mixer and the VGA produce 2nd-order nonlinear distortion on to the signal band. Thus, it is sufficient to consider only these two components when deriving the total power of the 2nd-order nonlinear distortion. Furthermore, all the components are assumed to produce 3rd-order nonlinear distortion.

A.1 Derivation

The derivation is done with linear power units to present the calculations in a more compact form. The total power of the signal at the input of the receiver chain is denoted as p_{in}. It consists of the signal of interest, SI, and thermal noise. The increase in the thermal noise power occurring within the receiver chain is omitted, as it has no significant effect on the power of the nonlinear distortion. Using (4.7), and expressing the output power in terms of gain and input power, the power of the 3rd-order nonlinear distortion at the output of the LNA can now be written as

$$P_{\text{3rd,LNA}} = G_{\text{LNA}} + P_{\text{in}} - 2(IIP3_{\text{LNA}} - P_{\text{in}}) \tag{A.1}$$

Using the linear units, this can be correspondingly written as

$$p_{\text{3rd,LNA}} = \frac{g_{\text{LNA}} p_{\text{in}}^3}{iip3_{\text{LNA}}^2}. \tag{A.2}$$

Now, noting that with the chosen parameters the power of the nonlinear distortion is negligibly small in comparison to the total power of the signal, the input power for the mixer can be written as

$$p_{\text{in,mixer}} = g_{\text{LNA}} p_{\text{in}} + p_{\text{3rd,LNA}} \approx g_{\text{LNA}} p_{\text{in}}. \tag{A.3}$$

The power of the 2nd-order nonlinear distortion produced by the mixer can then be written as

$$p_{\text{2nd,mixer}} = \frac{g_{\text{mixer}} p_{\text{in,mixer}}^2}{iip2_{\text{mixer}}} = \frac{g_{\text{mixer}}}{iip2_{\text{mixer}}} \left(g_{\text{LNA}} p_{\text{in}}\right)^2 = \frac{g_{\text{LNA}}^2 g_{\text{mixer}} p_{\text{in}}^2}{iip2_{\text{mixer}}}. \tag{A.4}$$

The power of the 3rd-order nonlinear distortion produced by the mixer can in turn be written as

$$p_{3\mathrm{rd,mixer}} = \frac{g_{\mathrm{mixer}} p_{\mathrm{in,mixer}}^3}{iip3_{\mathrm{mixer}}^2} = \frac{g_{\mathrm{mixer}}}{iip3_{\mathrm{mixer}}^2} \left(g_{\mathrm{LNA}} p_{\mathrm{in}}\right)^3 = \frac{g_{\mathrm{LNA}}^3 g_{\mathrm{mixer}} p_{\mathrm{in}}^3}{iip3_{\mathrm{mixer}}^2}. \tag{A.5}$$

Again, noting that the power of the nonlinear distortion is negligibly small in comparison to the total power of the signal, the input power of the VGA can be written as

$$p_{\mathrm{in,VGA}} \approx g_{\mathrm{mixer}} p_{\mathrm{in,mixer}} \approx g_{\mathrm{LNA}} g_{\mathrm{mixer}} p_{\mathrm{in}}. \tag{A.6}$$

The power of the 2nd-order nonlinear distortion at the output of the VGA can thus be written as

$$p_{2\mathrm{nd,VGA}} = \frac{g_{\mathrm{VGA}} p_{\mathrm{in,VGA}}^2}{iip2_{\mathrm{VGA}}} = \frac{g_{\mathrm{VGA}}}{iip2_{\mathrm{VGA}}} \left(g_{\mathrm{LNA}} g_{\mathrm{mixer}} p_{\mathrm{in}}\right)^2 = \frac{g_{\mathrm{LNA}}^2 g_{\mathrm{mixer}}^2 g_{\mathrm{VGA}} p_{\mathrm{in}}^2}{iip2_{\mathrm{VGA}}}. \tag{A.7}$$

Similarly, the power of the 3rd-order nonlinear distortion at the output of the VGA can be written as

$$p_{3\mathrm{rd,VGA}} = \frac{g_{\mathrm{VGA}} p_{\mathrm{in,VGA}}^3}{iip3_{\mathrm{VGA}}^2} = \frac{g_{\mathrm{VGA}}}{iip3_{\mathrm{VGA}}^2} \left(g_{\mathrm{LNA}} g_{\mathrm{mixer}} p_{\mathrm{in}}\right)^3 = \frac{g_{\mathrm{LNA}}^3 g_{\mathrm{mixer}}^3 g_{\mathrm{VGA}} p_{\mathrm{in}}^3}{iip3_{\mathrm{VGA}}^2}. \tag{A.8}$$

Finally, the total power of the nonlinear distortion of each order can be determined by summing up the powers of the nonlinear distortion at the output of each individual component. Thus, the total power of the 2nd-order nonlinear distortion can be written as follows, using (A.4) and (A.7):

$$\begin{aligned} p_{2\mathrm{nd}} &= g_{\mathrm{VGA}} p_{2\mathrm{nd,mixer}} + p_{2\mathrm{nd,VGA}} = g_{\mathrm{VGA}} \frac{g_{\mathrm{LNA}}^2 g_{\mathrm{mixer}} p_{\mathrm{in}}^2}{iip2_{\mathrm{mixer}}} + \frac{g_{\mathrm{LNA}}^2 g_{\mathrm{mixer}}^2 g_{\mathrm{VGA}} p_{\mathrm{in}}^2}{iip2_{\mathrm{VGA}}} \\ &= g_{\mathrm{LNA}}^2 g_{\mathrm{mixer}} g_{\mathrm{VGA}} p_{\mathrm{in}}^2 \left(\frac{1}{iip2_{\mathrm{mixer}}} + \frac{g_{\mathrm{mixer}}}{iip2_{\mathrm{VGA}}}\right). \end{aligned} \tag{A.9}$$

Similarly, the total power of the 3rd-order nonlinear distortion can be written as follows, using (A.2), (A.5), and (A.8):

$$\begin{aligned} p_{3\mathrm{rd}} &= g_{\mathrm{mixer}} g_{\mathrm{VGA}} p_{3\mathrm{rd,LNA}} + g_{\mathrm{VGA}} p_{3\mathrm{rd,mixer}} + p_{3\mathrm{rd,VGA}} \\ &= g_{\mathrm{mixer}} g_{\mathrm{VGA}} \frac{g_{\mathrm{LNA}} p_{\mathrm{in}}^3}{iip3_{\mathrm{LNA}}^2} + g_{\mathrm{VGA}} \frac{g_{\mathrm{LNA}}^3 g_{\mathrm{mixer}} p_{\mathrm{in}}^3}{iip3_{\mathrm{mixer}}^2} + \frac{g_{\mathrm{LNA}}^3 g_{\mathrm{mixer}}^3 g_{\mathrm{VGA}} p_{\mathrm{in}}^3}{iip3_{\mathrm{VGA}}^2} \\ &= g_{\mathrm{LNA}} g_{\mathrm{mixer}} g_{\mathrm{VGA}} p_{\mathrm{in}}^3 \left[\left(\frac{1}{iip3_{\mathrm{LNA}}}\right)^2 + \left(\frac{g_{\mathrm{LNA}}}{iip3_{\mathrm{mixer}}}\right)^2 + \left(\frac{g_{\mathrm{LNA}} g_{\mathrm{mixer}}}{iip3_{\mathrm{VGA}}}\right)^2\right]. \end{aligned} \tag{A.10}$$

A.2 Error analysis

In order to arrive with a relatively simple form for the powers of the nonlinearities, certain approximations are made in the derivation process of (A.9) and (A.10). Firstly, the increase in the thermal noise floor caused by each of the components is omitted from the equations. Secondly, it is observed that with realistic parameters, certain terms are negligibly small. These terms are thus omitted from the equations.

Due to these approximations, there is some error in the power values that are obtained with the derived equations. In order to quantify the amount of the error, the difference between the correct power value and the approximated value is calculated with respect to transmit power. This difference is then divided by the correct power value to obtain the relative error.

The error calculated by this method is illustrated in Fig. A.1 for Case A and Parameter Set 1. It is observed that this scenario produces the highest error, and it is thus analyzed here. From the figure, it can be seen that the error is smaller with higher transmit powers. This is an important feature, as the RX nonlinearities are negligibly weak with low transmit powers, and thus any small error in their values is insignificant. With transmit powers above 5 dBm, the error can be observed to be below 0.7 %. With lower transmit powers, the RX nonlinearities need not to be considered, and thus a small error does not matter.

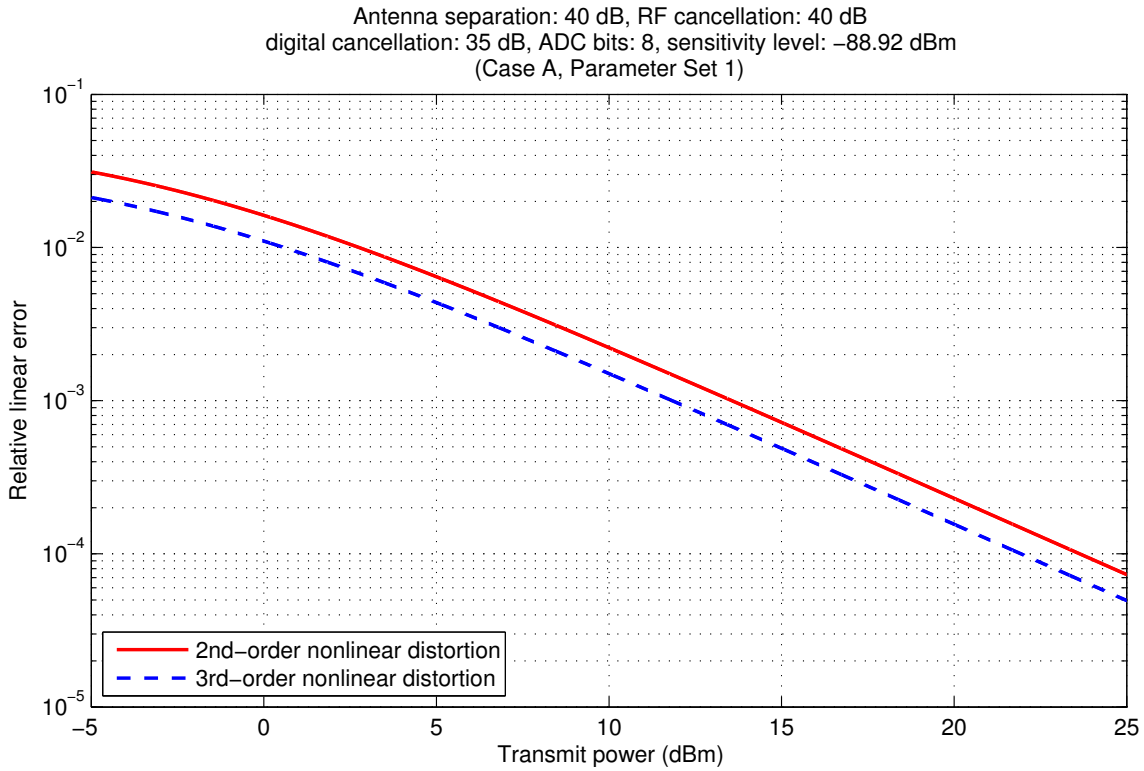

Figure A.1: Relative error of the values calculated with (4.14) and (4.15).

B. DERIVATION OF BIT LOSS DUE TO SELF-INTERFERENCE

A principal equation for the bit loss due to noise and interference is written in (4.18). However, as we are now interested in the amount of bits lost due to SI, the bit losses under HD and FD operation must be compared. By subtracting the amount of lost bits under HD operation from the amount of lost bits under FD operation, a value for bit loss due to SI is obtained. The equation for the bit loss is thus written as

$$b_{\text{lost}} = \frac{P_{\text{target}} - P_{\text{SOI,FD}}}{6.02} - \frac{P_{\text{target}} - P_{\text{SOI,HD}}}{6.02}, \tag{B.1}$$

where P_{target} corresponds to the total power of the signal at the input of the ADC (which is always constant because of AGC), and $P_{\text{SOI,FD}}$ and $P_{\text{SOI,HD}}$ are the powers of the signal of interest with and without SI, respectively. Because the total power of the signal at the input of the ADC is kept constant by the AGC, (B.1) can be further simplified to express the bit loss in terms of the gains:

$$b_{\text{lost}} = \frac{P_{\text{SOI,HD}} - P_{\text{SOI,FD}}}{6.02} = \frac{P_{\text{SOI,in}} + G_{\text{HD}} - (P_{\text{SOI,in}} + G_{\text{FD}})}{6.02} = \frac{G_{\text{HD}} - G_{\text{FD}}}{6.02}, \tag{B.2}$$

where G_{FD} is the total gain of the receiver chain under FD operation, and G_{HD} is the total gain under HD operation, correspondingly. This is a rather intuitive expression for the bit loss, as the power of SI is obviously included in G_{FD} due the reduction of the gain by the AGC. Noting that $G = P_{\text{target}} - P_{in}$ and $6.02 \approx 10\log_{10}(4)$, the bit loss can be now rewritten as

$$\begin{aligned} b_{\text{lost}} &= \frac{(P_{\text{target}} - P_{\text{in,HD}}) - (P_{\text{target}} - P_{\text{in,FD}})}{10\log_{10}(4)} = \frac{P_{\text{in,FD}} - P_{\text{in,HD}}}{10\log_{10}(4)} = \frac{10\log_{10}\left(\frac{p_{\text{in,FD}}}{p_{\text{in,HD}}}\right)}{10\log_{10}(4)} \\ &= \log_4\left(\frac{p_{\text{in,FD}}}{p_{\text{in,HD}}}\right) \approx \log_4\left(\frac{p_{\text{SOI,in}} + p_{\text{N,in}} + p_{\text{SI,in}} + p_{\text{3rd,PA,in}}}{p_{\text{SOI,in}} + p_{\text{N,in}}}\right) \\ &= \log_4\left(1 + \frac{p_{\text{SI,in}} + p_{\text{3rd,PA,in}}}{p_{\text{SOI,in}} + p_{\text{N,in}}}\right). \end{aligned} \tag{B.3}$$

By denoting that $p_{\text{SI,in}} = \frac{p_{\text{tx}}}{a_{\text{ant}}a_{\text{RF}}}$ and $p_{\text{3rd,PA,in}} = \frac{p_{\text{3rd,PA,tx}}}{a_{\text{ant}}a_{\text{NL}}} = \frac{p_{\text{tx}}^3}{a_{\text{ant}}a_{\text{NL}}iip3_{\text{PA}}^2 g_{\text{PA}}^2}$, (B.3) can finally be written as follows:

$$b_{\text{lost}} = \log_4\left[1 + \left(\frac{1}{p_{\text{SOI,in}} + p_{\text{N,in}}}\right)\left(\frac{p_{\text{tx}}}{a_{\text{ant}}a_{\text{RF}}} + \frac{p_{\text{tx}}^3}{a_{\text{ant}}a_{\text{NL}}iip3_{\text{PA}}^2 g_{\text{PA}}^2}\right)\right]. \tag{B.4}$$